

Synthesis, structure, transformation studies and catalytic properties of open-framework cadmium thiosulfate compounds†

Avijit Kumar Paul,^a Giridhar Madras^{*b} and Srinivasan Natarajan^{*a}

Received 7th May 2009, Accepted 2nd November 2009

First published as an Advance Article on the web 12th January 2010

DOI: 10.1039/b908995k

Five new thiosulfate based inorganic–organic hybrid open-framework compounds have been synthesized employing mild reaction conditions. Of the five compounds, $[\text{Na}_2(\text{H}_2\text{O})_8]\text{Cd}(\text{C}_{10}\text{H}_8\text{N}_2)(\text{S}_2\text{O}_3)_2 \cdot 2\text{H}_2\text{O}$, **I** and $[\text{Cd}_2(\text{C}_{10}\text{H}_8\text{N}_2)_2(\text{HS}_2\text{O}_3)_2(\text{S}_2\text{O}_3)_2][(\text{C}_{10}\text{H}_9\text{N}_2)_2(\text{C}_{10}\text{H}_8\text{N}_2)_2] \cdot 8\text{H}_2\text{O}$, **II** have one-dimensional (1D) structures and $[\text{Cd}(\text{C}_{10}\text{H}_8\text{N}_2)(\text{H}_2\text{O})_2(\text{S}_2\text{O}_3)] \cdot 2\text{H}_2\text{O}$, **III**, $[\text{Cd}_2(\text{C}_{10}\text{H}_8\text{N}_2)_3(\text{S}_2\text{O}_3)_2]$, **IV** and $[\text{Cd}_2(\text{C}_{10}\text{H}_8\text{N}_2)_{2.5}(\text{S}_2\text{O}_3)_2]$, **V** have three-dimensional (3D) structures. The 1D structures are somewhat related, formed by the bonding between tetrahedral Cd centers (CdN_2S_2) and 4,4'-bipyridine (bpy) units. The inter-chain spaces are occupied by the hanging thiosulfate units in both the cases along with $\text{Na}(\text{H}_2\text{O})_6$ chains in **I** and free bpy units in **II**. The three 3D structures have one-dimensional cadmium thiosulfate chains linked by bpy units. Interpenetration has been observed in all the 3D structures. The 3D structures appear to be related and can be derived from fgs net. Transformation studies on the 1D compound, $[\text{Na}_2(\text{H}_2\text{O})_8][\text{Cd}(\text{C}_{10}\text{H}_8\text{N}_2)(\text{S}_2\text{O}_3)_2] \cdot 2\text{H}_2\text{O}$, **I**, indicated a facile formation of $[\text{Cd}(\text{C}_{10}\text{H}_8\text{N}_2)(\text{H}_2\text{O})_2(\text{S}_2\text{O}_3)] \cdot 2\text{H}_2\text{O}$, **III**. Prolonged heating of **I** gave rise to a 3D cadmium sulfate phase, $[\text{Cd}_2(\text{C}_{10}\text{H}_8\text{N}_2)_2(\text{H}_2\text{O})_3(\text{SO}_4)_2] \cdot 2\text{H}_2\text{O}$, **VI**. Compound **VI** has one-dimensional cadmium sulfate chains formed by six-membered rings connected by bpy units to form a 3D structure, which appears to resemble the topological arrangement of **III**. Transformation studies of **III** indicates the formation of **IV** and **V**, and at a higher temperature a new 3D cadmium sulfate, $[\text{Cd}(\text{C}_{10}\text{H}_8\text{N}_2)(\text{SO}_4)]$, **VII**. Compound **VII** has a 4×4 grid cadmium sulfate layers pillared by bpy units. All the compounds were characterized by PXRD, TGA, IR and UV-visible studies. Preliminary studies on the possible use of the 3D compounds (**III–VII**) in heterogeneous cyanosilylation of imines appear to be promising.

Introduction

Inorganic open-framework compounds are an important class of solids, which have attracted much attention due to their important potential applications in the areas of sorption, separation and catalysis.¹ Most of the open-framework solids investigated and reported in the literature pertains to the silicates and the phosphates.² Recently, it has been shown that the oxy-anions of sulfur and selenium can also form open networks.³ One of the important issues with regards to the sulfate and selenate anions compared to the phosphate and silicate ones, is the difference in the formal oxidation state of the central atom, which would lead to an increased charge on the X–O–M bonds (X = Si, P, S, Se and M = metal atom) within the framework. In addition, it is well known that the sulfates and the selenates do not readily form polymerisable ring structures, unlike the phosphates and the silicates. It has been suggested that the sulfates can form stable structures with low valent metal ions. Persistent research during

the last few years has yielded several organic amine templated open-framework metal sulfates.³

Generally the open-framework structures are formed by bonding between the metal oxygen polyhedra and the anion tetrahedra, which essentially have M–O–X type bonding only. It seemed rational to examine whether such open-framework compounds can be prepared by employing a tetrahedral anion that contain more than one ligand, *viz.*, thiosulfate (S_2O_3)^{2–}.

One of the problems with the thiosulfate is its lack of stability under acidic conditions. Many of the open-framework compounds are prepared under acidic conditions employing hydrothermal methods.² The thiosulfate anion (S_2O_3)^{2–} has sulfur both in the +6 as well as in the –2 oxidation states, which renders the (S_2O_3)^{2–} ion unstable. So, under the reaction conditions, the thiosulfate decomposes to form elemental sulfur (generally as cyclic S_8 polymorph) or reacts further giving rise to metal sulfides. The other possibility would be that the thiosulfate decomposes forming either the sulfite or the sulfate anions, which eventually react with the metal ions to form the corresponding phases. Thus, the low stability of the thiosulfate anion creates a slight impediment for the synthetic chemist and could be the reason for the lack of open-framework thiosulfate phases in the literature.

The low stability coupled with the lack of reactivity of the thiosulfate anion necessitates newer approaches in the synthesis. Since the sulfates predominantly form low-dimensional structures, it is expected that the thiosulfate would also form similar ones. It has also been shown that the use of thiosulfate under mild

^aFramework Solids Laboratory, Solid State and Structural Chemistry Unit, Indian Institute of Science, Bangalore-560012, India. E-mail: snatarajan@sscu.iisc.ernet.in

^bDepartment of Chemical Engineering, Indian Institute of Science, Bangalore-560012, India. E-mail: giridhar@chemeng.iisc.ernet.in

† Electronic supplementary information (ESI) available: Experimental data. CCDC reference numbers 697711–697713 and 727266–727269. For ESI and crystallographic data in CIF or other electronic format see DOI: 10.1039/b908995k

conditions gives rise to one-dimensional structures.⁴ Increasing the dimensionality of a solid has been elegantly established by Lii and coworkers by the use of 4,4'-bipyridine as a rigid linker in many open-framework structures.⁵ We explored the preparation of the thiosulfate phases by employing reaction conditions that facilitates self assembly as well as solvothermal methods in combination with the use of 4,4'-bipyridine in the reaction mixture. We have chosen cadmium as the element of choice as it is likely to bind with sulfur more easily due to its larger size. We have employed self assembly approaches (room temperature or lower) to study the possible evolution of structures as a function of temperature. Such studies in MOF compounds exhibit profound effects in both the dimensionality as well as structures.⁶ This combined strategy yielded new inorganic–organic hybrid phases with thiosulfate as part of the network structure.⁷ In the present study, we have prepared five thiosulfate based hybrid compounds of varying dimensionalities. The compounds, $[\text{Na}_2(\text{H}_2\text{O})_8][\text{Cd}(\text{C}_{10}\text{H}_8\text{N}_2)(\text{S}_2\text{O}_3)_2] \cdot 2\text{H}_2\text{O}$, **I** and $[\text{Cd}_2(\text{C}_{10}\text{H}_8\text{N}_2)_2(\text{HS}_2\text{O}_3)_2(\text{S}_2\text{O}_3)_2][(\text{C}_{10}\text{H}_9\text{N}_2)_2(\text{C}_{10}\text{H}_8\text{N}_2)_2] \cdot 8\text{H}_2\text{O}$, **II** have one-dimensional structures, and $[\text{Cd}(\text{C}_{10}\text{H}_8\text{N}_2)(\text{H}_2\text{O})_2(\text{S}_2\text{O}_3)] \cdot 2\text{H}_2\text{O}$, **III**, $[\text{Cd}_2(\text{C}_{10}\text{H}_8\text{N}_2)_3(\text{S}_2\text{O}_3)_2]$, **IV** and $[\text{Cd}_2(\text{C}_{10}\text{H}_8\text{N}_2)_{2.5}(\text{S}_2\text{O}_3)_2]$, **V** have three-dimensional structures. Two three-dimensional sulfate based compounds $[\text{Cd}_2(\text{C}_{10}\text{H}_8\text{N}_2)_2(\text{H}_2\text{O})_3(\text{SO}_4)_2] \cdot 2\text{H}_2\text{O}$, **VI**, and $[\text{Cd}(\text{C}_{10}\text{H}_8\text{N}_2)(\text{SO}_4)]$, **VII**, have also been isolated during the study of the interconversion of the thiosulfate compounds. The structure of the cadmium sulfate compound $[\text{Cd}_2(\text{C}_{10}\text{H}_8\text{N}_2)_2(\text{H}_2\text{O})_3(\text{SO}_4)_2] \cdot 2\text{H}_2\text{O}$, **VI**, was already known, though with different water content.⁸ In this paper, we describe the synthesis, structure, transformation studies and heterogeneous catalytic properties of the thiosulfate phases.

Results and discussion

Structure of $[\text{Na}_2(\text{H}_2\text{O})_8][\text{Cd}(\text{C}_{10}\text{H}_8\text{N}_2)(\text{S}_2\text{O}_3)_2] \cdot 2\text{H}_2\text{O}$, **I**

The asymmetric unit contains 35 non-hydrogen atoms. The crystallographically independent Cd centers are tetrahedrally coordinated by two sulfur atoms of the thiosulfate unit and two nitrogen atoms of the 4,4'-bipyridine (CdN_2S_2 , $\text{CN} = 4$). The asymmetric unit contains two thiosulfate units, both of which are disordered over two positions with a site occupancy of 70 : 30 (see ESI†). The average S–S and S–O bond distances are 1.991 and 1.462 Å, respectively. The thiosulfate unit possesses an average angle of 106.1° , which is indicative of a distorted tetrahedral arrangement. The N–Cd–N bond angle is $84.9(2)^\circ$, and the S(1A)–Cd–S(2A) bond angle is $103.8(1)^\circ$. The structure of **I** consists of one-dimensional chains formed by the linking of cadmium centers by bipyridine units (Fig. 1(a)). The 4,4'-bpy units are twisted around the central C–C bond with an average torsion angle of 60.0° . The two thiosulfate units are bonded with the Cd through Cd–S linkages and hang as a pendent from the chain in the inter-chain region. The anionic chains are separated by the presence of one-dimensional cationic chains formed by the sodium atoms, which are octahedrally coordinated and bonded together by the water molecules (Fig. 1(b)). The interesting point about this structure is, while the anionic cadmium thiosulfate chains propagate along the “b” axis, the sodium–water chain propagates along the “a” axis (Fig. 1(c)). Thus, the two chains

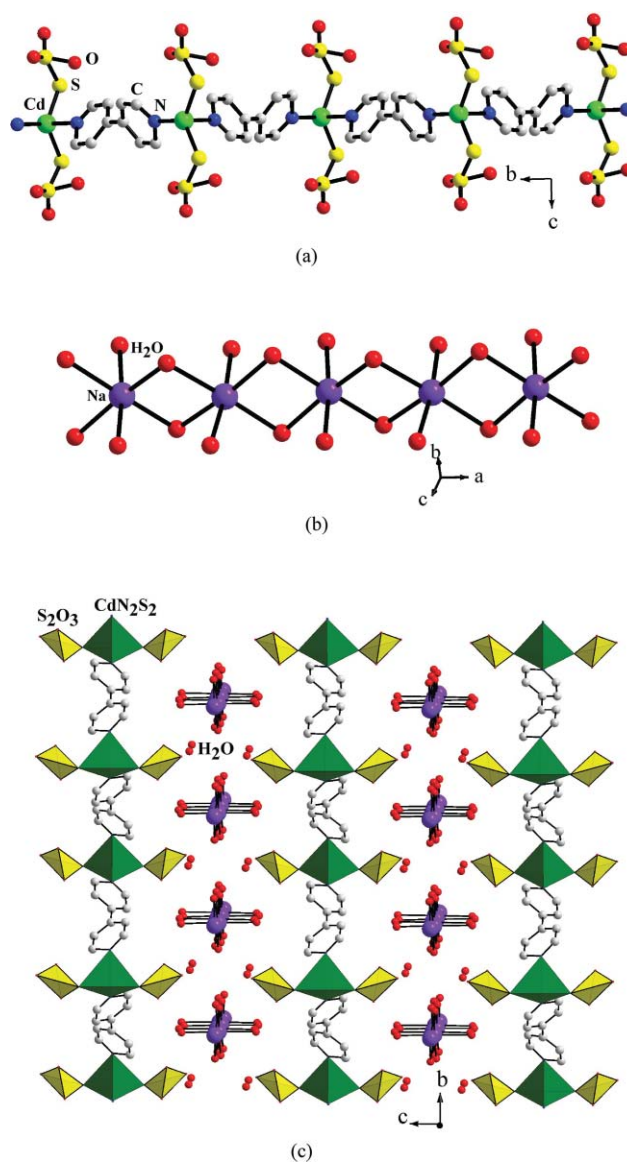


Fig. 1 (a) One-dimensional structure of $[\text{Na}_2(\text{H}_2\text{O})_8][\text{Cd}(\text{C}_{10}\text{H}_8\text{N}_2)(\text{S}_2\text{O}_3)_2] \cdot 2\text{H}_2\text{O}$, **I**. Note that the thiosulfate unit hangs from the Cd-center. Only one sulfur atom and the oxygen atoms (S1A, S2A, O2B, O3B, O4B and O5B; 70% occupancy) of each thiosulfate unit have been shown for clarity. (b) One-dimensional sodium–water chain observed in **I**. (c) The structure of **I** showing the arrangement of the anionic and the cationic chains. Note that the cationic chains propagate orthogonal to the Cd-bpy chains (see text). The hydrogen atoms of the bpy units and the water molecules are omitted in the figures for clarity.

are orthogonal to each other and the spaces between the chains are occupied by the water molecules. The presence of $[\text{Na}(\text{H}_2\text{O})_4]_n$ chains, water molecules and terminal S=O units in close proximity in **I** indicates the possibility of strong hydrogen bond interactions. Since, we could not locate the hydrogen positions of the water molecules from the single-crystal study, it was not possible to evaluate the nature and strength of the hydrogen bond interactions. The O–O distances, however, can provide some clues to the possible nature of such interactions. Thus, we have average O–O distances of 2.78 Å between the $[\text{Na}(\text{H}_2\text{O})_4]_n$ chains and the

lattice water molecules, 2.77 Å between the S=O and the water molecules, and 2.65 Å between the S=O and $[\text{Na}(\text{H}_2\text{O})_4]_n$ chains. These are typical distances that indicates strong hydrogen bond interactions.⁹

Structure of $[\text{Cd}_2(\text{C}_{10}\text{H}_8\text{N}_2)_2(\text{HS}_2\text{O}_3)_2(\text{S}_2\text{O}_3)_2][(\text{C}_{10}\text{H}_5\text{N}_2)_2-(\text{C}_{10}\text{H}_8\text{N}_2)_2]\cdot 8\text{H}_2\text{O}$, **II**

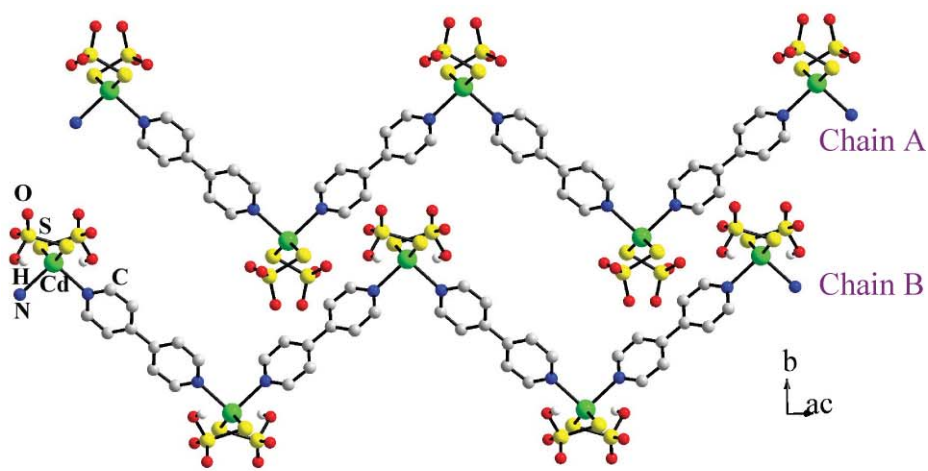
The asymmetric unit contains 52 non-hydrogen atoms. There are two crystallographically distinct cadmium ions and both occupy special positions (2f and 2e) with a site multiplicity of 0.5. Both the cadmium ions are tetrahedrally coordinated with two sulfur from the thiosulfate units and two nitrogen atoms from the 4,4'-bipyridine units (CdN_2S_2 , CN = 4). The Cd–N and Cd–S bond distances have an average value of 2.346 and 2.486 Å, respectively. The two thiosulfate units have average S–S and S–O bond distances of 2.029 and 1.464 Å, respectively. The thiosulfate unit has an average angle of 109.4°, which is indicative of a regular tetrahedral arrangement. The N–Cd–N bond angles are in the range 94.0(2)–94.5(2)° and the S–Cd–S bond angles are in the range 142.5(1)–144.4(1)°. Compound **II** also has a one-dimensional structure formed by the linking of the cadmium centers by the bipyridine units, similar to **I** (Fig. 2(a)). The C–C bond of the 4,4'-bipyridine, in **II**, is not twisted and the torsion angle is only 1.4° between the two benzene rings. The thiosulfate units in **II** have both protonated and deprotonated species and are bonded with cadmium through the monodentate sulfur atom. Out of two distinct cadmium centers, one is coordinated exclusively with two $(\text{HS}_2\text{O}_3)^-$ units while the other is coordinated with two $(\text{S}_2\text{O}_3)^{2-}$. This gives rise to two distinct chains, which are stacked alternatively in the “*ab*” plane (Fig. 2(a)). The $(\text{HS}_2\text{O}_3)^-$ and $(\text{S}_2\text{O}_3)^{2-}$ units hang as a pendent in the inter-chain region from the cadmium center. The structure of **II** also possesses two free 4,4'-bipyridine molecules, one of which is protonated, and occupies the inter-chain spaces along with four lattice water molecules. The bonding of two $(\text{S}_2\text{O}_3)^{2-}$ units with the cadmium center renders one of the one-dimensional chains anionic, which is neutralized by the protonated bpy unit. It may be noted that the position of the bpy molecules in **II** is similar to the arrangement of the one-dimensional sodium–water chain in **I** (Fig. 2(b)). The free 4,4'-bipyridine units are twisted around the central C–C bond with an average torsion angle of 27.4°. The twisting of the free bpy appears to maximize the interactions with the lattice water molecules. Here, we have both N–H⋯N and C–H⋯O interactions. The possible O–H⋯O and O–H⋯N interactions in this structure could not be evaluated as we have not been successful in finding the actual positions of the hydrogen atoms bound with the lattice water molecules. The N⋯N (donor–acceptor) distance between the protonated end and the free end of the bpy is 2.74(1) Å and the N–H⋯N bond angle is 175.0°, suggesting favorable hydrogen bond interactions, paving the formation of a dimer. Similarly, the C⋯O distances are in the range 3.24(1)–3.45(1) Å while the C–H⋯O bond angles are in the range 155.0–173.0°. The observed O⋯N and O⋯O distances are in the range 2.60(1)–2.78(1) Å. The O⋯O and O⋯N interactions appear to be strong in this structure also and the C–H⋯O interactions can provide active secondary supporting role.^{9b}

Structure of $[\text{Cd}(\text{C}_{10}\text{H}_8\text{N}_2)(\text{H}_2\text{O})_2(\text{S}_2\text{O}_3)]\cdot 2\text{H}_2\text{O}$, **III**

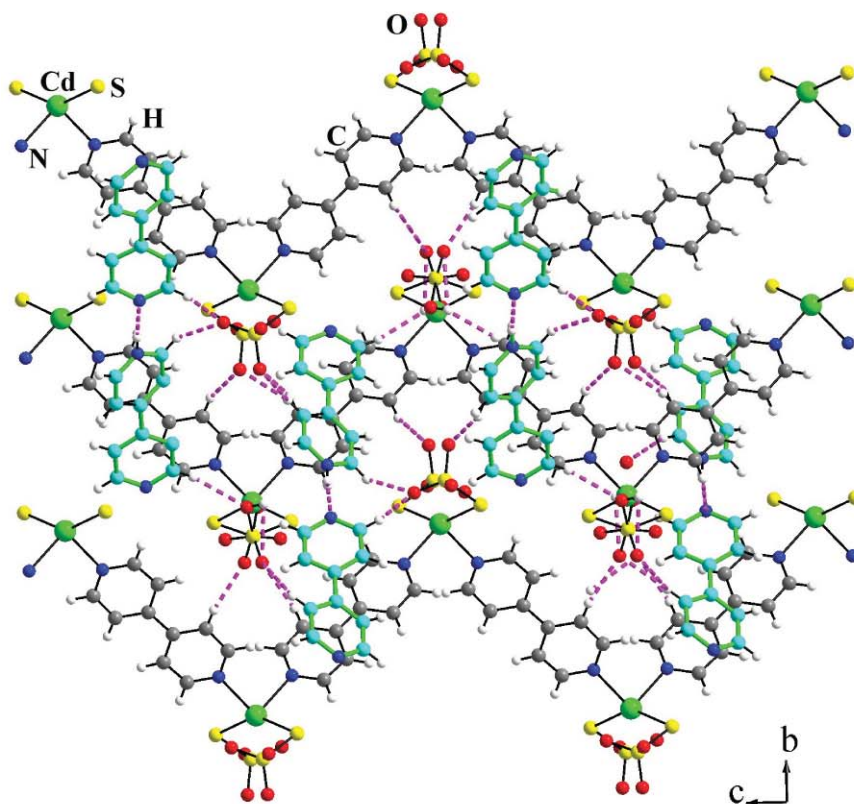
The asymmetric unit of **III** contains 22 non-hydrogen atoms. There is only one crystallographically independent Cd^{2+} ion, which is coordinated by one sulfur and one oxygen atom of the thiosulfate unit, two nitrogen atoms of the bipyridine and two terminal water molecules forming a distorted octahedral environment, ($\text{Cd}(\text{H}_2\text{O})_2\text{N}_2\text{SO}$, CN = 6). The average Cd–N and Cd–O bond distances are 2.324 and 2.350 Å, respectively. The Cd–S bond distance is 2.644 (1) Å. The thiosulfate has average S–O bond distances of 1.445 and the S–S bond distance is 2.016 Å. The thiosulfate unit has an average angle of 109.5°, which is typical for the tetrahedral arrangement. The O/S–Cd–S/O bond angles are in the range 95.66(8)–173.75(9)° and the N–Cd–N bond angle is 176.61(11)°. The Cd center is connected with one sulfur and one oxygen from two different thiosulfate units and forms a one-dimensional chain, which is arranged as a right handed helix (Fig. 3(a)). The 4,4'-bipyridine units link the chain by bonding with the Cd-centers completing the three-dimensional connectivity. The 4,4'-bipyridine connectivity is such that only the alternate Cd centers are linked to form the two-dimensional layer like arrangement (Fig. 3(b)). The two-dimensional layers interpenetrate each other forming the three-dimensional structure (Fig. 3(c)). The most important aspect of the structure is that all the bpy units are planar and the central C–C bonds are not twisted. There are two extra-framework water molecules in the asymmetric unit and two other water molecules are generated by the symmetry, which occupy the middle of the one-dimensional channels. The water molecules form a cyclic tetrameric cluster arrangement with an average distance of 2.78 Å (Fig. 3(d)) between the water molecules, which is often observed in many hybrid compounds including MOFs.¹⁰

Structure of $[\text{Cd}_2(\text{C}_{10}\text{H}_8\text{N}_2)_3(\text{S}_2\text{O}_3)_2]$, **IV**

The asymmetric unit of **IV** contains 25 non-hydrogen atoms. There are two crystallography independent Cd^{2+} ions, Cd(1) and Cd(2), both occupying special positions (4e) with a site multiplicity of 0.5. The Cd(1) is coordinated by two oxygen atoms from two thiosulfate units and four nitrogen atoms from the 4,4'-bipyridine units forming a distorted octahedral environment ($\text{Cd}(1)\text{N}_4\text{O}_2$, CN = 6) and Cd(2) is coordinated by two sulfur atoms from the thiosulfate units and two nitrogen atoms from the 4,4'-bipyridine units forming a tetrahedral environment ($\text{Cd}(2)\text{N}_2\text{S}_2$, CN = 4). The average Cd–N, Cd–O and Cd–S bond distances are 2.352, 2.307 and 2.524 Å, respectively. The thiosulfate unit has an average S–O bond distance of 1.454 and S–S bond distance of 2.044 Å. The thiosulfate unit has an average angle of 109.4°, which is indicative of the tetrahedral arrangement. The O–Cd–O bond angle is 177.3(1)°, the S–Cd–S bond angle is 103.9(1)° and the N–Cd–N bond angles are in the range 93.02(9)–167.50(8)°. The structure of **IV** consists of the connectivity involving the tetrahedral and the octahedral Cd centers, the thiosulfate unit and the 4,4'-bipyridine unit. Thus, the tetrahedral and the octahedral Cd centers are connected through the thiosulfate units to form a one-dimensional chain structure (Fig. 4(a)). The cadmium thiosulfate chains are bonded with the 4,4'-bipyridine units giving rise to the three-dimensional structure. The octahedral and the tetrahedral Cd centers from the



(a)



(b)

Fig. 2 (a) One-dimensional structure of $[\text{Cd}_2(\text{C}_{10}\text{H}_8\text{N}_2)_2(\text{HS}_2\text{O}_3)_2(\text{S}_2\text{O}_3)_2][(\text{C}_{10}\text{H}_8\text{N}_2)_2(\text{C}_{10}\text{H}_8\text{N}_2)_2] \cdot 8\text{H}_2\text{O}$, **II**. Note that two $(\text{S}_2\text{O}_3)^{2-}$ units hang from the Cd-center of chain A and two $(\text{HS}_2\text{O}_3)^-$ units hang from the Cd-center of chain B. The hydrogen atoms are omitted for clarity. (b) The structure of **II** showing the arrangement of the Cd-bpy chains along with the free bpy molecules. Dotted lines represent possible hydrogen bond interactions and the free bpy units have been shown in a different color.

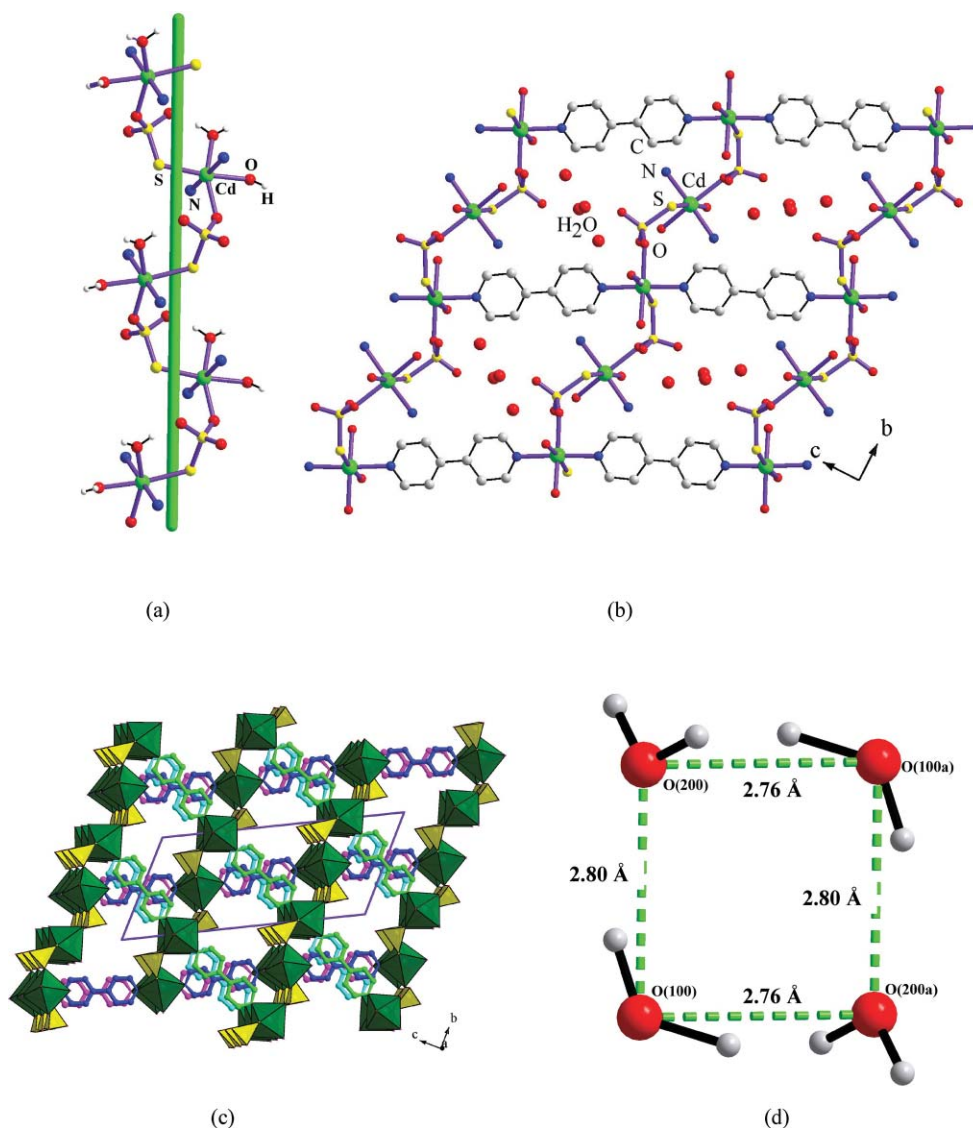


Fig. 3 (a) The one-dimensional cadmium thiosulfate helical chain in $[\text{Cd}(\text{C}_{10}\text{H}_8\text{N}_2)(\text{H}_2\text{O})_2(\text{S}_2\text{O}_3)] \cdot 2\text{H}_2\text{O}$, **III**. (b) Figure shows the connectivity between the adjacent chains through the bpy units in the bc plane forming the two-dimensional layer arrangement. (c) The three-dimensional structure of **III**. The different colors of the bpy units indicate connectivity between two different layers. The hydrogen atoms of bpy and water are omitted for clarity. (d) The cyclic water tetramer found in the channels in **III**.

adjacent chains are connected through the bpy units forming a two-dimensional layer (Fig. 4(b)) where the bpy units are twisted around the central C–C bond with an average torsion angle of 11.3° . The other nitrogen coordination of the octahedral Cd centers are utilized to form the three-dimensional structure *via* bonding with 4,4'-bipyridine units (Fig. 4(c)) which are not twisted around the central C–C bond. In this structure interpenetration is also observed.

Structure of $[\text{Cd}_2(\text{C}_{10}\text{H}_8\text{N}_2)_{2.5}(\text{S}_2\text{O}_3)_2]$, **V**

The asymmetric unit of **V** contains 42 non-hydrogen atoms. There are two crystallography independent Cd^{2+} ions and both occupy normal positions. The Cd(1), is tetrahedrally coordinated by two sulfur and two nitrogen atoms ($\text{Cd}(1)\text{N}_2\text{S}_2$, $\text{CN} = 4$), and Cd(2) is coordinated by two oxygen atoms and three nitrogen atoms

to form a distorted trigonal bipyramidal (TBP) environment ($\text{Cd}(2)\text{N}_3\text{O}_2$, $\text{CN} = 5$). The average Cd–N, Cd–O and Cd–S bond distances are 2.321, 2.326 and 2.491 Å, respectively. The average S–O and S–S bond distances in the thiosulfate are 1.443 and 2.060 Å, respectively. The thiosulfate unit has an average angle of 109.4° . The O–Cd–O bond angle is $75.2(1)^\circ$, the S–Cd–S bond angle is $119.2(1)^\circ$ and the N–Cd–N bond angles are in the range of $88.01(9)$ to $173.59(10)^\circ$. The strictly alternating tetrahedral and TBP Cd centers are connected through the thiosulfate unit forming one-dimensional cadmium thiosulfate chains (Fig. 5(a)). The cadmium thiosulfate one-dimensional chains are connected by the 4,4'-bipyridine units forming the three-dimensional structure. The tetrahedral and TBP Cd centers from the adjacent chains are connected through the bpy units to form the two-dimensional layer (Fig. 5(b)). Here, the layer is formed by two different bpy units with an average torsion angle of 24.7° and 3.1° around the central C–C

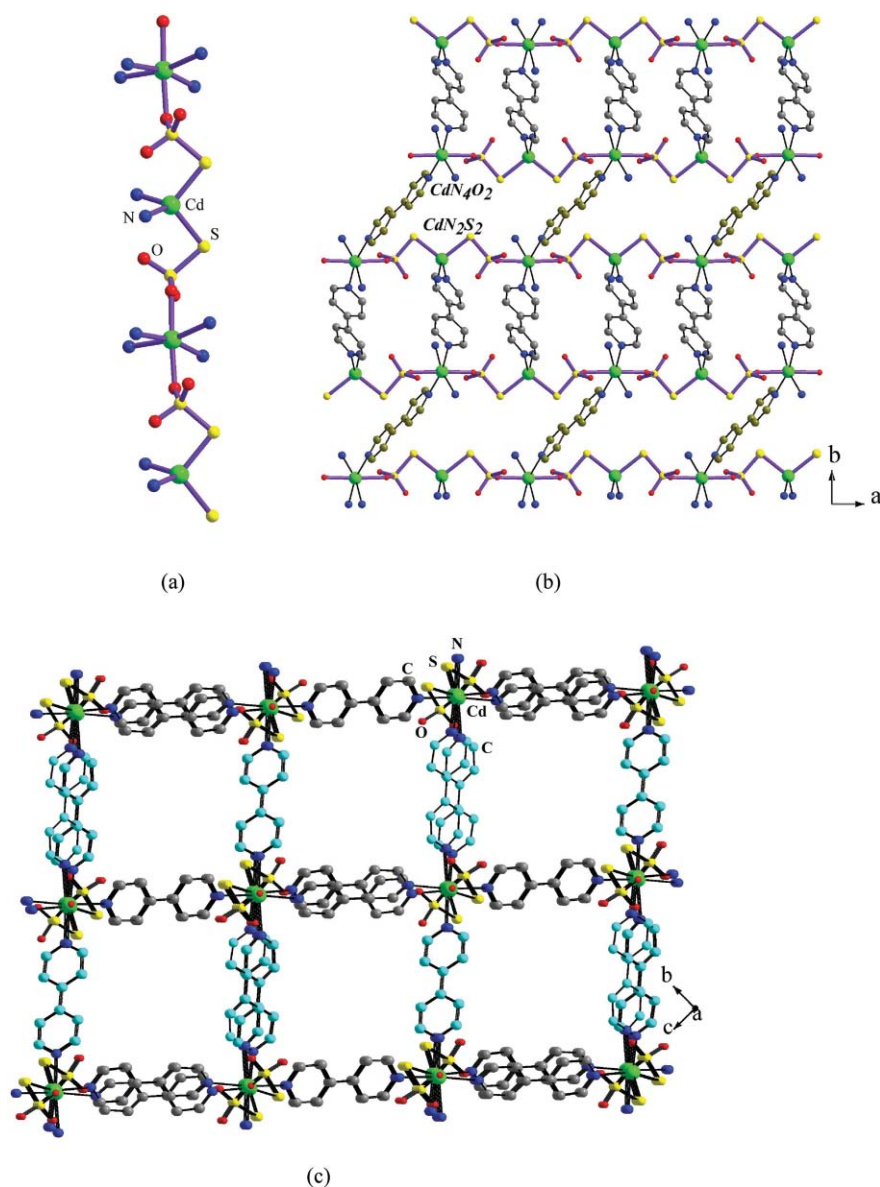


Fig. 4 (a) The one-dimensional cadmium thiosulfate chain in $[Cd_2(C_{10}H_8N_2)_3(S_2O_3)_2]$, **IV**. (b) Figure shows the connectivity between the chains by the bpy units in the *ab* plane. (c) The three-dimensional structure of **IV**. The hydrogen atoms of the bpy units are omitted for clarity.

bond. The one extra nitrogen coordination of TBP Cd centers is utilized to form the three-dimensional structure (Fig. 5(c)) where the bpy units are not twisted around the central C–C bond. In this structure we also observed interpenetration similar to that observed in **IV**.

Structural comparison

Among all the cadmium thiosulfate phases prepared in the present study, **I** and **II** have one-dimensional structures, whereas **III**, **IV** and **V** have three-dimensional structures. All the structures have connectivity that involves cadmium ions, thiosulfate and bipyridine units. The Cd centers have different coordination environments. The one-dimensional structures of **I** and **II** are formed by the connectivity between the tetrahedral cadmium and bpy units. The thiosulfate units are not

part of the one-dimensional structural arrangement, but hang in the inter-chain spaces and participate in hydrogen bond interactions, which could lend some stability to these low-dimensional structures. The one-dimensional structures may also be compared with the earlier reported zinc thiosulfate structure, $\{[Zn(C_{10}H_8N_2)(H_2O)_4][Zn_2(S_2O_3)_3(C_{10}H_8N_2)_2] \cdot 2H_2O\}_n$.^{4a} The zinc thiosulfate compound is formed by the linking of zinc centers by bipyridine as well as the thiosulfate units (Fig. 6(a)). This gives rise to a double chain structure instead of a simple one-dimensional structure observed for **I** and **II**. The zinc thiosulfate compound also possesses one terminal thiosulfate unit, where both **I** and **II** have two terminal thiosulfate units. Similar to the zinc thiosulfate compound, **I** and **II** are also anionic. The charge compensation is achieved by the presence of $[Na(H_2O)_4]_n$ and protonated bipyridine units in **I** and **II**, respectively, whereas the $[Zn(bpy)(H_2O)_4]_n$ chain acts as the compensating unit in

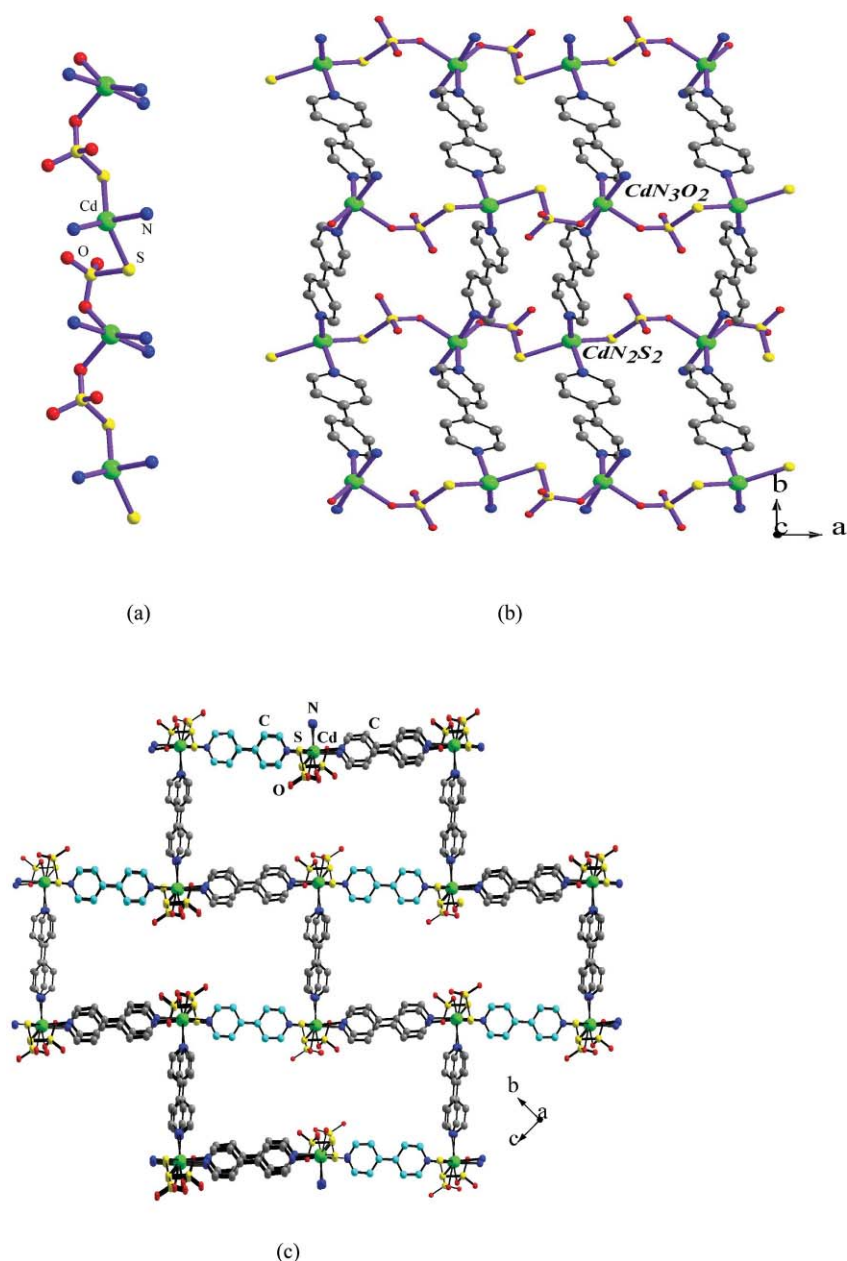


Fig. 5 (a) The one-dimensional cadmium thiosulfate chain in $[\text{Cd}_2(\text{C}_{10}\text{H}_8\text{N}_2)_{2.5}(\text{S}_2\text{O}_3)_2]$, **V**. (b) Figure shows the connectivity between the chains by the bpy units in the *ab* plane. (c) The three-dimensional structure of **V**. The hydrogen atoms of the bpy units are omitted for clarity.

the reported structure.^{4a} A closer examination also reveals that the positions of the $[\text{Na}(\text{H}_2\text{O})_4]_n$ and bpy units in **I** and **II** are comparable to the $[\text{Zn}(\text{bpy})(\text{H}_2\text{O})_4]_n$ chains in the $\{[\text{Zn}(\text{C}_{10}\text{H}_8\text{N}_2)(\text{H}_2\text{O})_4][\text{Zn}_2(\text{S}_2\text{O}_3)_3(\text{C}_{10}\text{H}_8\text{N}_2)_2] \cdot 2\text{H}_2\text{O}\}_n$ compound (Fig. 6(b)). In the zinc thiosulfate structure, the $[\text{Zn}(\text{bpy})(\text{H}_2\text{O})_4]_n$ chains are mutually perpendicular (two chains), which is observed in **II** but not in **I** (Fig. 6(c) and 6(d)). The one-dimensional structures have close structural features to that reported earlier.^{4a}

The cadmium thiosulfate chains observed in the three-dimensional structures, **III**, **IV** and **V**, have also been observed in a manganese thiosulfate compound, $[\text{Mn}(\text{S}_2\text{O}_3)_2(\text{C}_{12}\text{H}_8\text{N}_2)(\text{H}_2\text{O})_2]$.^{4c} In the manganese thiosulfate compound, the use of 1,10-phenanthroline resulted in a simple chain structure

supported by $\pi \cdots \pi$ interactions (see ESI,† Fig. S12). In structures, **III**, **IV** and **V**, the use of 4,4'-bipyridine resulted in three-dimensional structures. The three-dimensional structures, **III**, **IV** and **V**, also have comparable structural features. The structures of the compounds have been reported recently by us.⁷ The three structures, however, appear to be related even though the coordination around the Cd atoms differ between them. The three 3D structures, **III**, **IV** and **V**, have interpenetrations arising primarily due to the connectivity involving the bpy units. We have performed a detailed structural analysis using the TOPOS40 program,¹¹ to understand the structural interpenetration in **III**, **IV** and **V**. The analysis indicated that compound **III** has cadmium thiosulfate chains cross-linking through the bpy units (Fig. 7(a)).

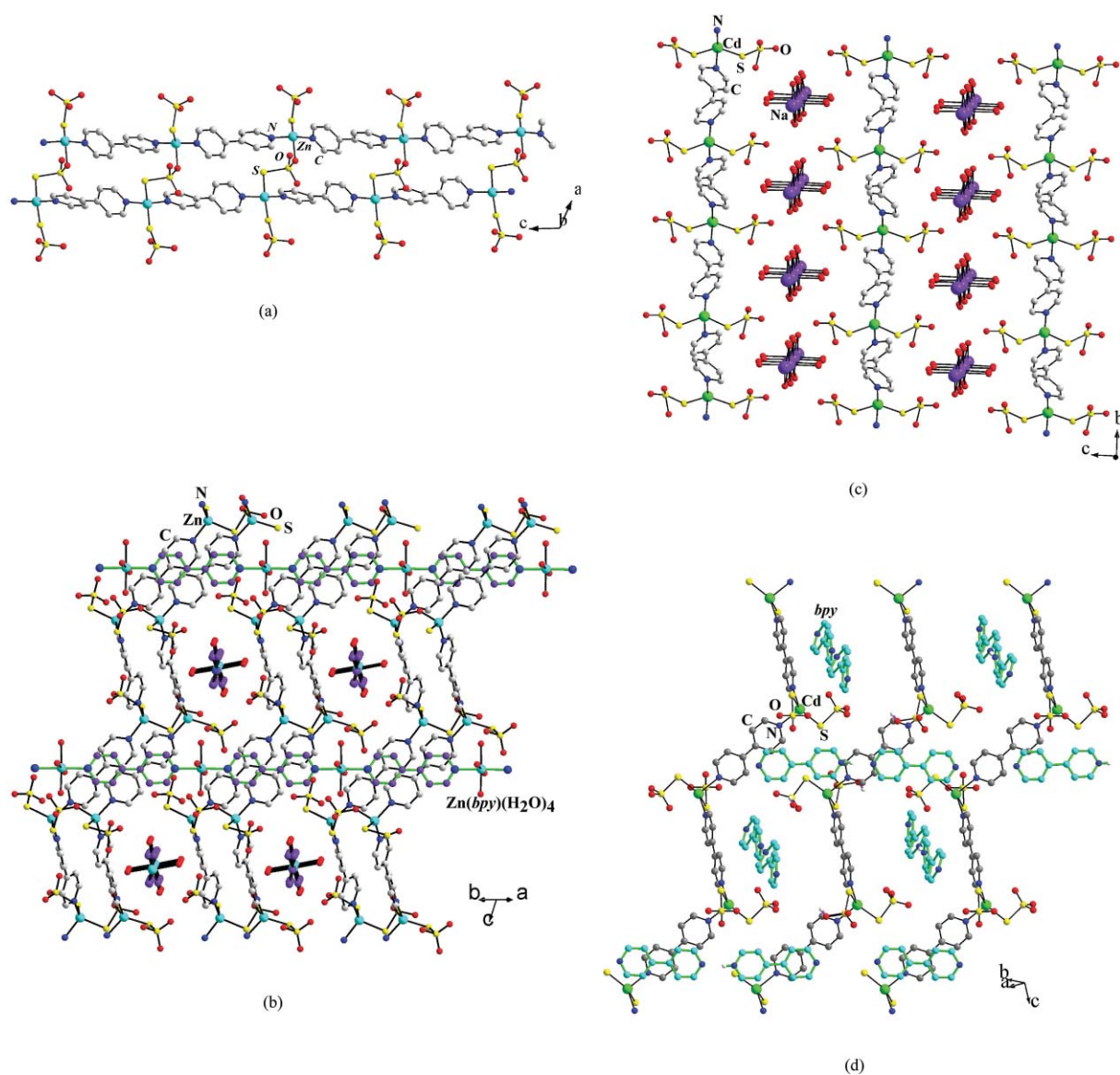


Fig. 6 (a) The zinc thiosulfate one-dimensional double-chain structure of $\{[\text{Zn}(\text{C}_{10}\text{H}_8\text{N}_2)(\text{H}_2\text{O})_4][\text{Zn}_2(\text{S}_2\text{O}_3)_3(\text{C}_{10}\text{H}_8\text{N}_2)_2] \cdot 2\text{H}_2\text{O}\}_n$. Note that the thiosulfate units hang from the Zn-center. (b) The packing diagram of $\{[\text{Zn}(\text{C}_{10}\text{H}_8\text{N}_2)(\text{H}_2\text{O})_4][\text{Zn}_2(\text{S}_2\text{O}_3)_3(\text{C}_{10}\text{H}_8\text{N}_2)_2] \cdot 2\text{H}_2\text{O}\}_n$. Note the presence of the zinc–water–bpy chains along the two mutually perpendicular directions. (c) View of the structure of **I** in the “bc” plane. (d) The packing diagram of compound **II**. Note that the free bipyridine units along the two mutually perpendicular directions. Note also the close structural similarity between the structures. Hydrogen atoms have been omitted for clarity.

A similar analysis on **IV** revealed the presence of two completely interpenetrated three-dimensional structures (Fig. 7(b), 7(c)). Each net that sustains the structure have similar building units (viewed along the *bc* plane) and the inter-penetration occurs only due to the bpy linkages between the two nets. The analysis of **V** also indicates the presence of two interpenetrated three-dimensional structures, but is different to **IV**. Here, the structure interpenetrates perpendicularly between the two three-dimensional structures (Fig. 7(d) and 7(e)), again mediated by the bpy units.

In addition to the interesting interpenetrations observed in the structures of **III**, **IV** and **V**, there are other structural relationships that exist between the three structures. All the three structures have different Cd : bpy ratios (1 : 1 in **III**, 1 : 1.5 in **IV** and 1 : 1.25 in **V**) but the Cd : S₂O₃ ratios are similar. This suggests close

structural relationships between the three structures. The presence of one-dimensional cadmium thiosulfate chains in **III–V** also suggests the possibility for structural relationships. The main difference between the structures arises due to the differences in the coordination geometry of the Cd centers. A careful study of the three structures suggested that they can be derived from the primitive cubic (pcu) structural network. The pcu net is generally based on an octahedrally connected structure (see ESI,† Fig. S13(a)). Of the three structures, only compound **III** contains octahedral Cd, but of the six connections, two are terminal water molecules, rendering the Cd centers as essentially four connected. Compound **IV**, on the other hand, has both octahedral as well as four-connected cadmium centers and can be used as the starting point to visualize the present structures as derived from the pcu

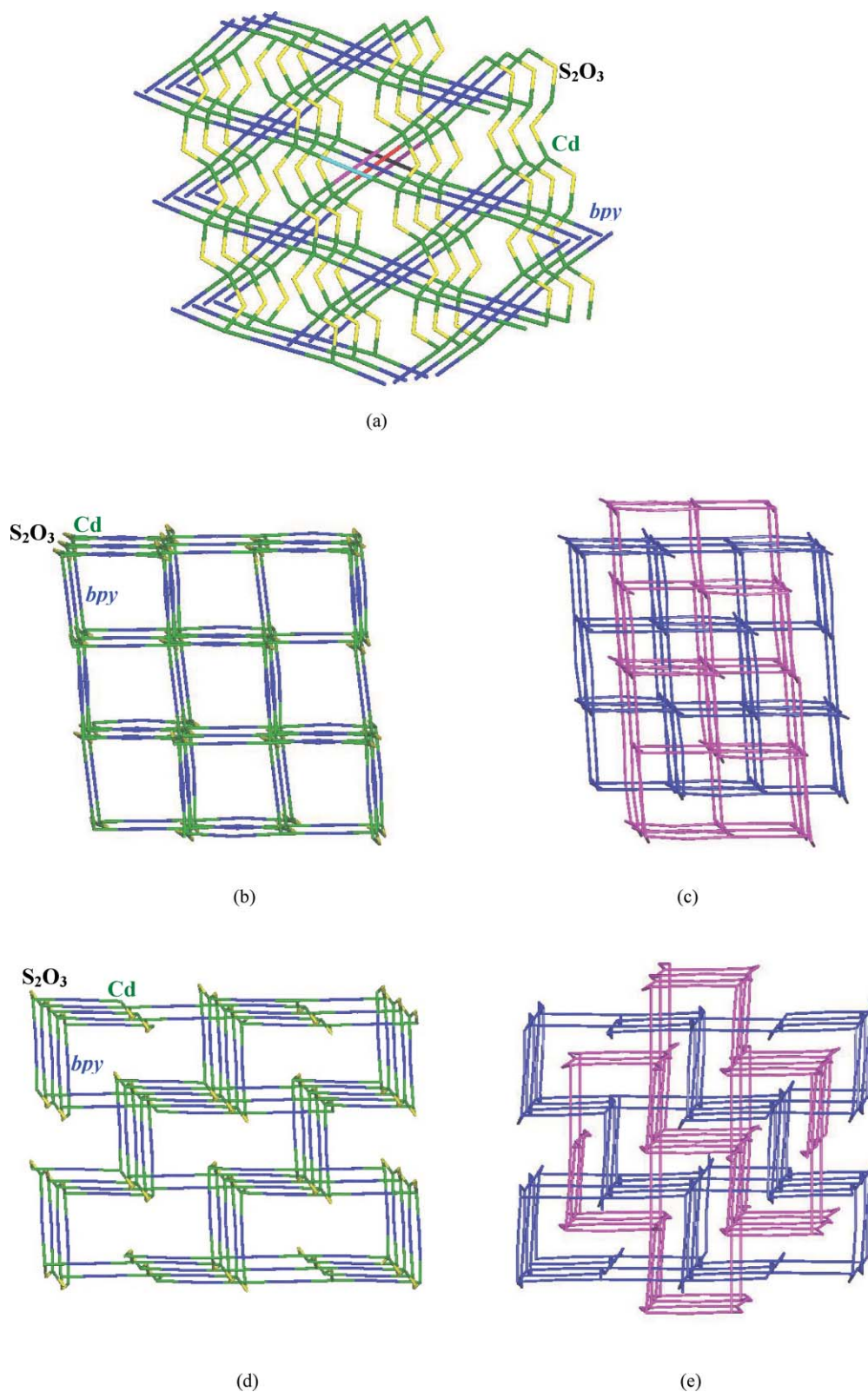


Fig. 7 (a) Figure shows the connectivity between the nodes (Cd centers) through the bpy and the S_2O_3 units in **III**. Note that the bpy units link the layers. (b) Figure shows the connectivity between the nodes (Cd centers) through the bpy and the S_2O_3 units in **IV**. Note that the connectivity forms a square-box like unit. (c) Figure shows the interpenetration observed in **IV**. Note that the two square grids interpenetrate perpendicularly (see text). (d) Figure shows the connectivity between the nodes (Cd centers) through the bpy and the S_2O_3 units in **V**. Note that the connectivity gives rise to a rectangular-box like unit. (e) Figure shows the interpenetration observed in **V**. Note that the rectangular-box units interpenetrate perpendicularly (see text).

net. It has been suggested that the combination of octahedral and four-coordinated metal centers can give rise to a pcu derived net known as the fgs net (see ESI,† Fig. S13(b)).¹² This fgs net has been observed earlier in $\text{Mn}_2(\text{dca})_3(\text{NO}_3)(\text{Mepyz})_2$.¹³ Our structure **IV** has similar connections to that of $\text{Mn}_2(\text{dca})_3(\text{NO}_3)(\text{Mepyz})_2$ and can be related to the fgs net. In **V**, we have four and five connected Cd centers, which could distort the fgs net further resulting in another derived net (see ESI,† Fig. S13(c)). Compound **III**, which essentially has only four-connections would further distort the fgs net (see ESI,† Fig. S13(d)). Thus, the three-dimensional thiosulfate structures **III**, **IV** and **V** are related and can be generated from the pcu net topology.

Transformation reactions

It has been shown earlier that the low-dimensional structures could be a precursor for structures of higher dimensionality.¹⁴ Since, in present compounds **I** and **II**, the low-dimensional structures do not have the continuous connectivity between the cadmium centers and the thiosulfate units, we believe that it would be interesting to examine the reactive nature of the 1D cadmium thiosulfate phases. Of the two compounds, **II** could not be obtained in pure form in large enough quantity for investigating the reactivity and hence only compound **I** was studied. For this, we have taken compound **I** and reacted at varying times and temperatures. The various experimental conditions employed for the transformation studies have been summarized in Table S9 (see ESI†).

For the transformation study, 0.18 g of **I** was heated in 2.4 ml of water at 30, 45 and 60 °C simultaneously in many closed containers. The reaction vessels were removed periodically at different time intervals, the products recovered by filtration and analyzed using powder X-ray diffraction (see ESI,† Fig. S14). As can be noted, compound **III** starts to form after about 12 h at 30 °C. The presence of compound **I** persists up to 48 h, after which we observe only compound **III**. On heating **I** at 45 °C, we observe the formation of compound **III** at about 6 h and compound **I** completely vanishes after 12 h. This suggests that **I** transforms to **III** at a much faster rate at elevated temperatures (45 °C compared to 30 °C). At 60 °C, though we observed a similar behavior of the formation of **III** after 6 h of reaction, at longer duration we observed the formation of **V**. Compound **III** persists up to 36 h and after that only the pure phase of **V** was observed. This suggests the possibility of **III** being an intermediate phase in the formation of **V**. In this context, it is worthwhile to note that we have prepared the pure phase of **III** at 30 °C in a water–ethanol mixture compared to 75 °C required to form **V** in pure water medium. Since compound **I** has been synthesized in a mixture of solvents (water–ethanol), we wanted to study the transformation of **I** in a water–ethanol mixture by employing similar conditions as before. For these set of reactions, we have taken 0.18 g of **I** in a solvent mixture containing 1.2 ml of water and 1.2 ml of ethanol (see ESI,† Fig. S15). The studies at 30 °C show the formation of **III** from **I**, but the trend is considerably different compared to that observed using only water as the solvent. Here, compound **III** starts to form even at 6 h and after 12 h there is no trace of **I** suggesting that the transformation of **I** to **III** is much more facile in a water–ethanol solvent mixture. At 45 °C, we do observe a similar trend, but in addition we also observe the formation of **V** during longer heating (after 36 h). This suggests that the

transformation reactions do proceed rapidly in a water–ethanol solvent mixture. The reactions carried out at 60 °C showed a completely different behavior and we observed newer peaks in the PXRD pattern (Fig. 8). As can be noted, we do not observe the formation of **III** at 60 °C, but **I** transforms directly to **V** after 6 h of heating at 60 °C. After 36 h, we observed new peaks, which were later identified as corresponding to the cadmium sulfate phase (compound **VI**). This suggests that the compound undergoes partial decomposition at elevated temperature in a water–ethanol mixture, with the $(\text{S}_2\text{O}_3)^{2-}$ unit losing some sulfur to form the $(\text{SO}_4)^{2-}$ units. The transformation reactions in a water–ethanol mixture also yielded good quality single-crystals of the new phase, which were employed for the structural studies. The single-crystal structural study showed that this phase is a cadmium sulfate $[\text{Cd}_2(\text{C}_{10}\text{H}_8\text{N}_2)_2(\text{H}_2\text{O})_3(\text{SO}_4)_2] \cdot 2\text{H}_2\text{O}$. The cadmium sulfate phase was prepared, subsequently, starting from individual components and is discussed later.

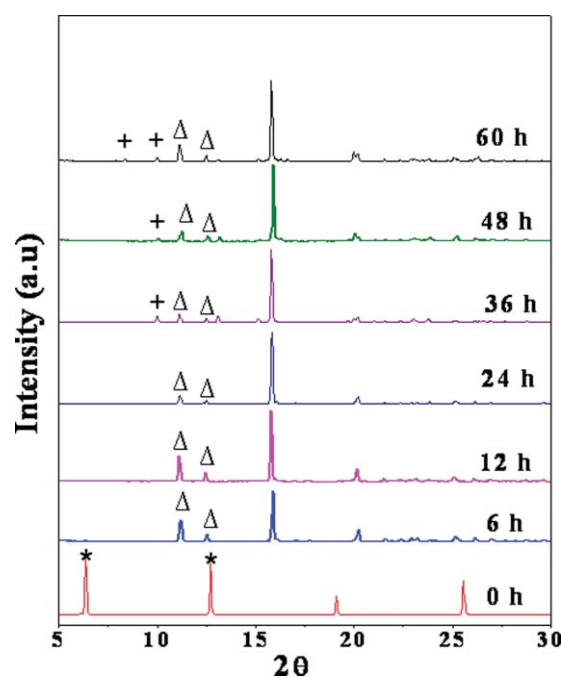


Fig. 8 Powder XRD pattern of the transformation reactions of **I** in a water–ethanol mixture at 60 °C. Note that the different phases start to form at different time intervals. (* = **I**, Δ = **V** and + = **VI**).

The transformation reactions confirmed the reactive nature of **I**. It is also possible to visualize the formation of structures **III** and **V** from **I** by simple manipulations (see ESI,† Scheme 1). The removal of the $(\text{S}_2\text{O}_3)^{2-}$ unit from **I** can form the simple two-dimensional layer observed in **III** and the further addition of bpy units can give rise to **V**. This indicates that the reaction pathway is not a simple solid state type reaction, but suggestive of the dissolution and recrystallization type reaction. Similar mechanistic pathways have been observed and postulated for the transformation reactions of one-dimensional zinc-phosphate phases.¹⁵

The transformation study of **I** suggested the possibility of **III** being an important intermediate in the formation of other cadmium thiosulfate phases. In addition, our structural evaluation also suggested that compound **III** has the most distorted structure when one derives from the pcu net. So, it occurred to us that

we could investigate the possible reactivity of **III**. The various experimental conditions employed for the transformation studies have been summarized in Table S10 (ESI).†

For the transformation studies, we have taken 0.15 gm of **III** and heated in water at 30, 45 and 60 °C (see ESI,† Fig. S16). At 30 °C, we did not observe any new products even after 60 h. The reactions at 45 °C, however, indicated the formation of compound **V** after 48 h but the transformation was not complete as compound **III** persisted up to 60 h. At 60 °C, the formation of **V** was seen after 24 h and compound **III** disappeared completely after 36 h. We did not observe any other phase other than **V** up to 60 h. These studies showed that **III**, indeed, transforms to another related phase (**V**) as a function of time and temperature. Since, the reactivity of **I** was observed to be much more facile in a water–ethanol mixture, we investigated the transformation of **III** in a water–ethanol mixture at 30, 45 and 60 °C following a similar procedure as described earlier (see ESI,† Fig. S17). The studies indicated that compound **III** did not undergo any transformations at 30 °C irrespective of the duration of the reaction. At 45 °C, compound **III** starts to transform to **V** after 12 h and the transformation was completed after 24 h. We did not observe the formation of any other phase up to 60 h. At 60 °C, the formation of compound **V** was observed within 6 h. After 24 h, we observed additional new phases in the PXRD, which corresponded to the cadmium sulfate phase observed during the transformation of **I** in a water–ethanol mixture at 60 °C. The transformation studies of **III** appear to confirm our view that **III** could be an intermediate and also support the results of the transformation reactions of **I**.

Since, the bpy:Cd ratio among all the three 3D compounds are different, we wanted to examine the possible conversion of **III** to **IV** and/or **V**, as the latter two have higher bpy/Cd ratios (1.5 and 1.25, respectively, compared to 1 : 1 for **III**). For this, **III** was reacted with stoichiometric quantities of bpy (0.25 and 0.5 mol) for varying times and temperatures. As before, the products were isolated and examined by PXRD studies (see ESI,† Fig. S18, S19). The results indicated that there was no reaction at 30 °C, but at 45 °C in the presence 0.5 mol bpy the formation of compound **IV** was seen after 8 h. Pure phase of **IV** was observed only after 20 h. Similarly, at 45 °C in the presence of 0.25 mol bpy, we observed the formation of both **IV** and **V** after 8 h. We did not observe the formation of any one of the pure phases (**IV** or **V**) even after 20 h when the reactions were carried out using 0.25 mol bpy. At 60 °C, both **IV** and **V** form after 4 h in the presence of 0.25 and 0.5 mol of bpy. The pure phase of **V** was obtained after 20 h when the reactions were carried out using 0.25 mol bpy, but only a mixture of **IV** and **V**, while using 0.5 mol bpy.

Since, we have derived the structures of **III**, **IV** and **V** from the fgs net, it can be very easily shown schematically how the addition of bpy to the most distorted structure **III** can be effected (see ESI,† Scheme 2). This must involve changes in the bonding as well as the coordination environment around Cd.

We have also carried out one set of experiments at elevated temperature (110 °C) to investigate the transformation of **III**. After 12 h, the sample becomes grossly amorphous and the XRD pattern (Fig. 9) matched with that of CdS with a particle size of ~100 nm. On heating further, we observed an entirely new phase. Few single crystals were found in the product after 48 h and the structural determination indicated that it is a cadmium sulfate phase, **VII**. This is the second cadmium sulfate phase

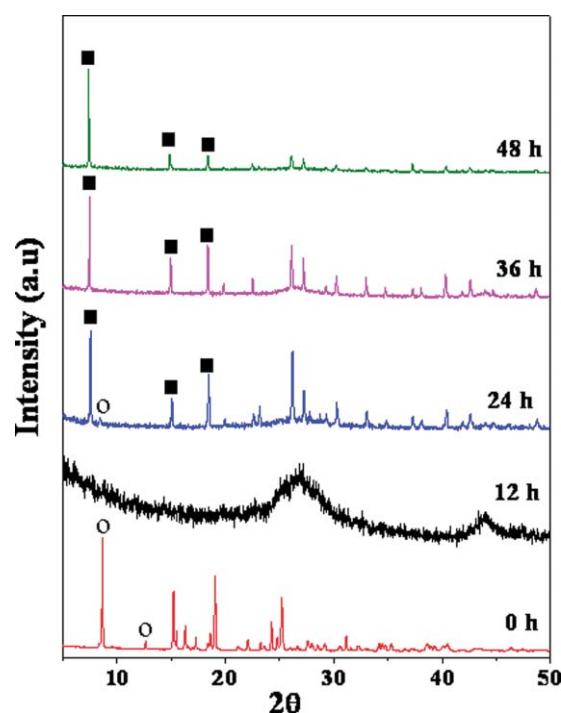
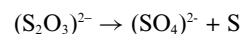


Fig. 9 Powder XRD pattern of the transformation reaction of **III** in ethanol medium at 110 °C (○ = **III**, ■ = **VII**).

that was isolated during the transformation reactions. From the transformation reactions, we believe the reaction proceeds *via* a dissolution and re-crystallization pathway. The formation of sulfate from thiosulfate is not surprising as the S–S bond is quite weak and tends to form the sulfate species under the reaction conditions.



The pathway can be substantiated as we observed the formation of sulfur (as S_8 species) and CdS phase. The results of the various transformation studies can be summarized schematically as shown in Scheme 1. The single-crystal study gave the stoichiometric compositions of the cadmium sulfate phases and we sought to prepare them starting from the individual components (Table 1).

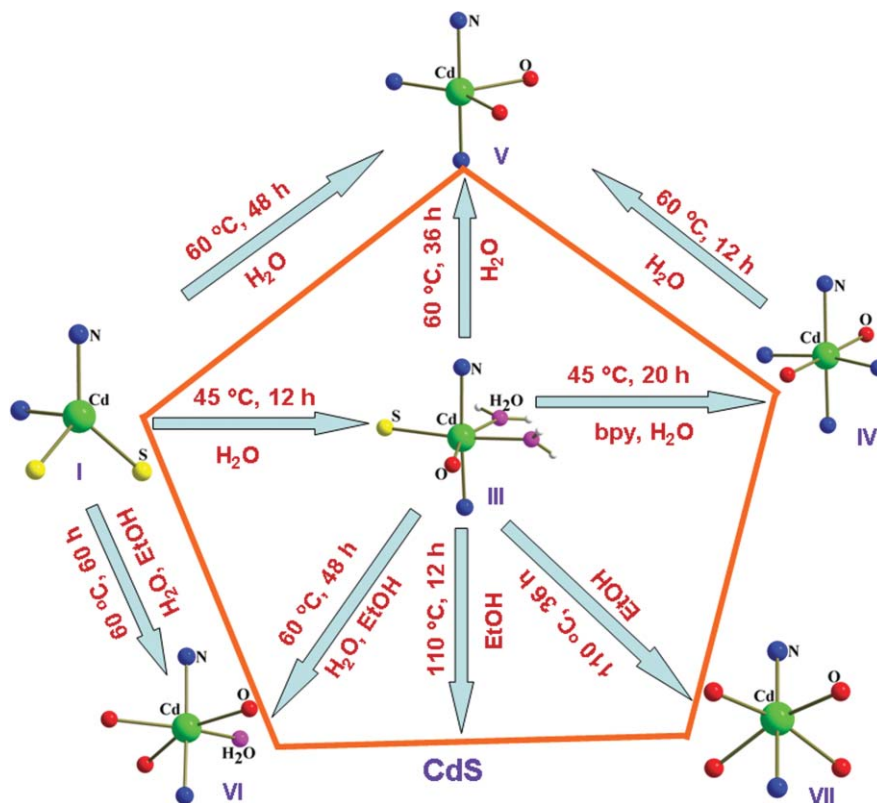
Structure of $[\text{Cd}_2(\text{C}_{10}\text{H}_8\text{N}_2)_2(\text{H}_2\text{O})_3(\text{SO}_4)_2] \cdot 2\text{H}_2\text{O}$, **VI**

The structure of compound **VI** is comparable to the cadmium sulfate $[\text{Cd}_2(\text{C}_{10}\text{H}_8\text{N}_2)_2(\text{H}_2\text{O})_3(\text{SO}_4)_2] \cdot 3\text{H}_2\text{O}$, reported previously.⁸ In the present structure, we observed less framework water molecules than the reported structure. Three CdO_4N_2 and SO_4 units are connected together forming a six-membered ring, which are further linked to form a one dimensional ladder-like chain along the “*b*” axis (Fig. 10(a)). The one-dimensional ladder-like units are connected by 4,4′-bipyridine ligands forming the three-dimensional structure (Fig. 10(b)). The structure of **VI** has features that are comparable to the structure of **III**, especially with regard to the bpy connectivity. The bpy connectivity in this structure has close resemblance to the interpenetration observed in **III**. The topological analysis, however, exhibits differences between the sulfate and thiosulfate chain in the structure **VI** and **III**, respectively (Fig. 10(c)).

Table 1 Synthetic compositions and conditions employed for compounds I–VII^a

S. No	Composition	Temp/°C	Time/h	pH (range)	Product	Yield (%)
1	1Cd(NO ₃) ₂ ·4H ₂ O + 2Na ₂ S ₂ O ₃ ·5H ₂ O + 1bpy + 51EtOH + 166H ₂ O	5	72	6.0–8.0	[Na ₂ (H ₂ O) ₈][Cd(C ₁₀ H ₈ N ₂)(S ₂ O ₃) ₂]·2H ₂ O, I	90
2	1Cd(NO ₃) ₂ ·4H ₂ O + 2Na ₂ S ₂ O ₃ ·5H ₂ O + 2bpy + 166H ₂ O	75	60	6.0	[Cd(C ₁₀ H ₈ N ₂)(HS ₂ O ₃) ₂][(C ₁₀ H ₈ N ₂) ₂]·4H ₂ O, II	70
3	1Cd(NO ₃) ₂ ·4H ₂ O + 2Na ₂ S ₂ O ₃ ·5H ₂ O + 1bpy + 51EtOH + 166H ₂ O	25	60	6.0–8.0	[Cd(C ₁₀ H ₈ N ₂)(H ₂ O) ₂ (S ₂ O ₃) ₂]·2H ₂ O, III	90
4	1Cd(NO ₃) ₂ ·4H ₂ O + 2Na ₂ S ₂ O ₃ ·5H ₂ O + 2bpy + 166H ₂ O	75	12–24	6.0–8.0	[Cd ₂ (C ₁₀ H ₈ N ₂) ₃ (S ₂ O ₃) ₂], IV	90
5	1Cd(NO ₃) ₂ ·4H ₂ O + 2Na ₂ S ₂ O ₃ ·5H ₂ O + 2bpy + 166H ₂ O	75	60	8.0	[Cd ₂ (C ₁₀ H ₈ N ₂) _{2.5} (S ₂ O ₃) ₂], V	85
6	1Cd(NO ₃) ₂ ·4H ₂ O + 1Na ₂ SO ₄ + 1bpy + 166H ₂ O	75	60	5.0	[Cd ₂ (C ₁₀ H ₈ N ₂) ₂ (H ₂ O) ₃ (SO ₄) ₂]·2H ₂ O, VI	90
7	1Cd(NO ₃) ₂ ·4H ₂ O + 1Na ₂ SO ₄ + 1bpy + 26EtOH + 83H ₂ O	110	60	5.0	[Cd(C ₁₀ H ₈ N ₂)(SO ₄)], VII	85

^a pH was adjusted by the addition of NH₄OH. Elemental analysis calcd (%) for **I**: C 16.69, H 3.89, N 2.78; found 16.48, H 3.96, N 2.88; Elemental analysis calcd (%) for **II**: C 40.94, H 3.87, N 9.55; found: C 40.81, H 3.69, N 9.48; Elemental analysis calcd (%) for **III**: C 26.50, H 3.53, N 6.18; found: C 26.54, H 3.54, N 6.15; Elemental analysis calcd (%) for **IV**: C 39.23, H 2.61, N 9.15; found: C 39.30, H 2.64, N 9.11; Elemental analysis calcd (%) for **V**: C 35.73, H 2.38, N 8.34; found: C 35.81, H 2.35, N 8.38; Elemental analysis calcd (%) for **VI**: C 29.29, H 3.17, N 6.83; found: C 29.44, H 3.11, N 6.88; Elemental analysis calcd (%) for **VII**: C 32.90, H 2.19, N 7.68; found: C 32.81, H 2.25, N 7.59.



Scheme 1 Scheme summarizing the transformation reactions. Only the Cd coordination sphere is shown for simplicity. Note that red atoms are the oxygen atoms of the thiosulfate and sulfate units. For compounds **IV**, **V** and **VI**, one Cd center has been shown for clarity.

Three-dimensional cadmium sulfate, VII, [Cd(C₁₀H₈N₂)(SO₄)]

The asymmetric unit contains 11 non-hydrogen atoms, of which one Cd and S are crystallographically independent. Both Cd and S occupy special positions (2c and 2b, respectively), with a site multiplicity of 0.25. The Cd atom is octahedrally coordinated with four oxygen atoms and two nitrogen atoms (CdN₂O₄), with

average Cd–O and Cd–N bond distances of 2.289 and 2.374 Å, respectively. The S atom is tetrahedrally coordinated by four oxygen atoms with an average S–O bond distance of 1.440 Å. The sulfate possesses an average O–S–O bond angle of 110.6°, which is indicative of the tetrahedral arrangement. The O–Cd–O bond angles are in the range 83.5(6)–160.8(1)° and the N–Cd–N bond angle is 180.0(1)°. The connectivity between CdN₂O₄ octahedra

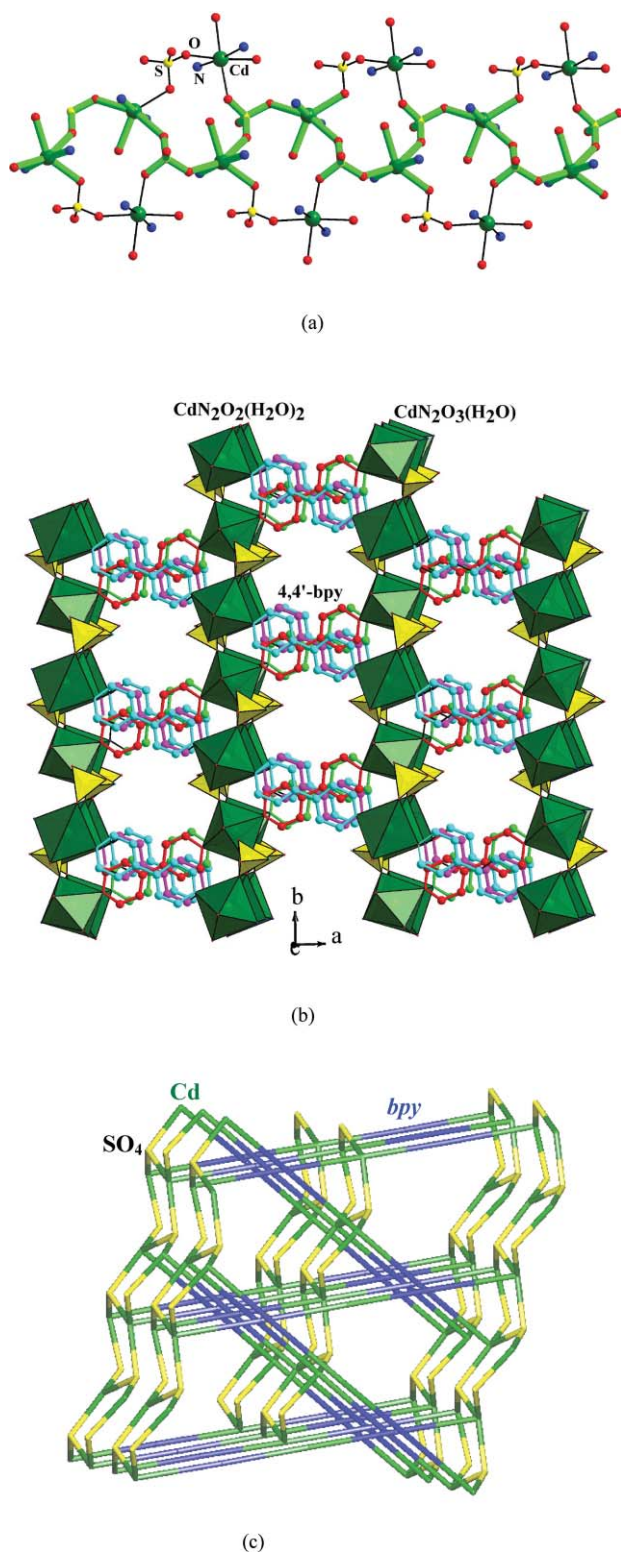


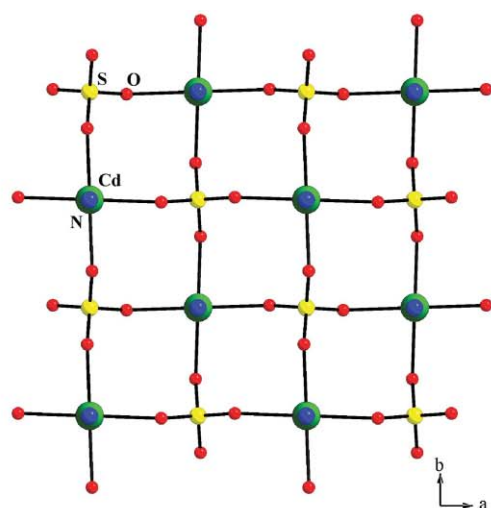
Fig. 10 (a) The one-dimensional cadmium sulfate chain observed in $[\text{Cd}_2(\text{C}_{10}\text{H}_8\text{N}_2)_2(\text{H}_2\text{O})_3(\text{SO}_4)_2] \cdot 2\text{H}_2\text{O}$, **VI**. Note that the chains are formed by the six-membered units. (b) The three-dimensional structure of **VI** showing the connectivity between the cadmium sulfate chains and the bpy units. The different colors of the bpy units indicate connectivity between two different layers. The hydrogen atoms of the bpy units are omitted for clarity. (c) Figure shows the connectivity between the chains and the bpy units. Note the similarity in the interpenetration with that of **III** (Fig. 6(a)).

and SO_4 tetrahedra give rise to a two-dimensional cadmium sulfate layers (Fig. 11(a)), which are pillared by the 4,4'-bipyridine units giving rise to the three-dimensional structure (Fig. 11(b)). The cadmium sulfate layers resemble a typical 4×4 square grid. From the topological point of view, the cadmium sulfate layers form the 4-4 nets (Fig. 11(c)) which are connected by bpy units.

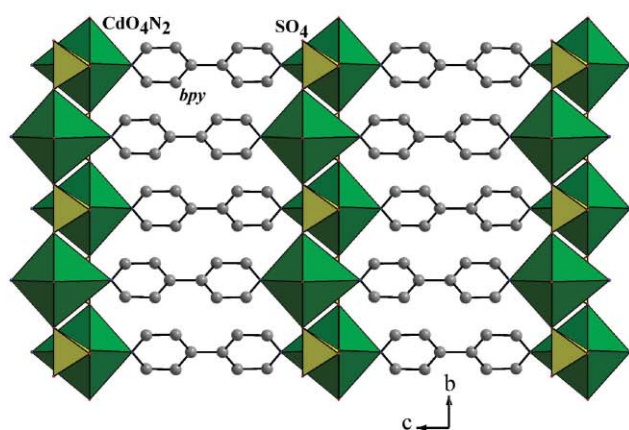
Both the cadmium sulfate structures, **VI** and **VII**, have three-dimensional connectivity involving the sulfate and the bipyridine unit. The bpy units connect the one-dimensional cadmium sulfate ladder-like units forming the 3D structure in **VI**, whereas it links a square grid cadmium sulfate layers in **VII**. The bpy connectivity of structure **VI** appears to have some resemblance to that found in **III**. The inorganic cadmium sulfate layer, observed in **VII**, has close resemblance to many similar structures reported in the literature. Thus, the cadmium sulfate layers are comparable to the two-dimensional layers observed in the zinc-arsenate, $\{[\text{C}_4\text{N}_2\text{H}_{12}][\text{Zn}(\text{AsO}_4)_2]\}$,¹⁶ and also with the cadmium sulfate layers in $\{[\text{H}_3\text{N}(\text{CH}_2)_3\text{NH}_3][\text{Cd}_2(\text{H}_2\text{O})_2(\text{SO}_4)_3]\}$ ¹⁷ (Fig. 12). The later structure has layers formed by the connectivity between CdO_6 octahedral and SO_4 tetrahedral units, but the presence of two terminal water molecules and a terminal sulfate unit reduces the Cd as a 4-connected center giving rise to the 4×4 grid (see ESI,† Fig. S20). Similarly, the gallium arsenate and phosphate structures $\{\text{Ga}_2(4,4'\text{-bpy})(\text{MO}_4)_2\}$, ($\text{M} = \text{As}, \text{P}$),¹⁸ have GaO_4N trigonal bipyramid units bound to MO_4 tetrahedra forming the 4×4 grid (see ESI,† Fig. S21). Since, the Ga-centers are only 5-coordinated the bipyridine units link only alternate Ga centers giving rise to the 3D structure. Thus, the layer in **VII** is comparable to many structures in the literature, but the connectivity between the layers gives rise to the observed differences.

Catalytic studies

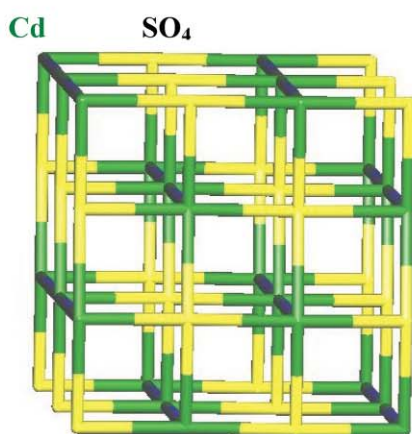
The formation of new types of structures in the family of inorganic–organic hybrids with thiosulfate as a component prompted us to investigate the efficacy of these solids for possible catalytic purposes. Recently, the cyanosilylation of imines has been carried out in the presence of $\{[\text{Cd}(4,4'\text{-bpy})_2(\text{H}_2\text{O})_2](\text{NO}_3)_2 \cdot 4\text{H}_2\text{O}\}_n$, heterogeneously.¹⁹ Since, the present compounds also involves bonding between the cadmium centers and the bipyridine units, we sought to perform a preliminary study of the catalytic reactivity of the 3D thiosulfate and sulfate compounds. For this, we employed similar experimental conditions as used in the earlier study.¹⁹ Typically a powdered catalyst (0.1 mmol) was suspended in CH_2Cl_2 solution (1.5 ml) of imine (**A**, 0.5 mmol). Trimethylsilyl cyanide (0.75 mmol) was added at 0°C and the reaction mixture was stirred for 1 h. The product, aminonitrile (**B**), was isolated and analyzed. Of the three 3D thiosulfate compounds, we found that compound **III** shows a quantitative conversion of the imine to the aminonitrile ($\sim 98\%$). Compounds **IV** and **V** show only about 40% conversion. The cadmium sulfate phases (**VI** and **VII**), on the other hand, exhibited a conversion of 60–63% (see ESI,† Table S12). In order to check the efficacy of the thiosulfate as the catalyst, we have also carried out control experiments in the absence of thiosulfate in the suspension. We did not observe any reaction between the reactants in the absence of catalysts. We have also carried out a similar experiment in the presence of $\text{Cd}(\text{NO}_3)_2 \cdot 4\text{H}_2\text{O}$, which gave a conversion of $\sim 20\%$. This suggests that the thiosulfates are active as the heterogeneous catalyst for



(a)

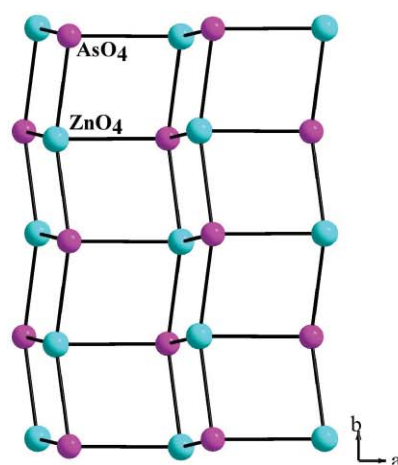


(b)

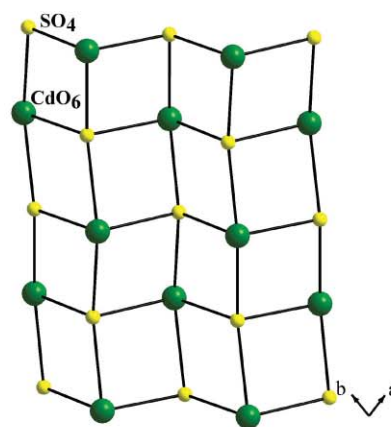


(c)

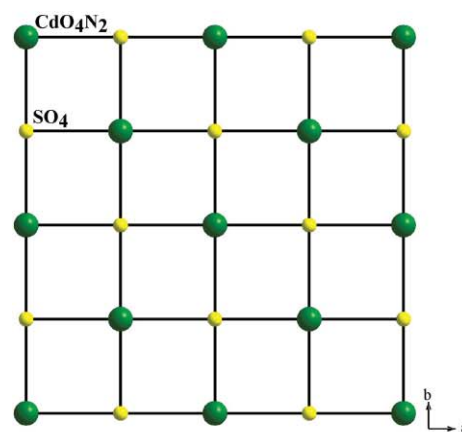
Fig. 11 (a) Figure shows the connectivity between CdO_4N_2 octahedra and SO_4 tetrahedra in $[\text{Cd}(\text{C}_{10}\text{H}_8\text{N}_2)(\text{SO}_4)]$, **VII**. Note the formation of a 4×4 two-dimensional square grid. (b) Figure shows the connectivity between the cadmium sulfate layers and the bpy units in **VII**. The hydrogen atoms of the bpy units are omitted for clarity. (c) Figure shows the connectivity between the nodes (Cd-center) through the SO_4 and the bpy units.



(a)



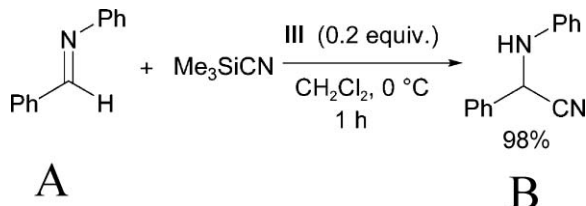
(b)



(c)

Fig. 12 (a) The two-dimensional 4×4 layer observed in the zinc-arsenate, $\{[\text{C}_4\text{N}_2\text{H}_{12}][\text{Zn}(\text{AsO}_4)_2]\}$. (b) The two-dimensional 4×4 layer observed in the cadmium-sulfate, $\{[\text{H}_3\text{N}(\text{CH}_2)_3\text{NH}_3][\text{Cd}_2(\text{H}_2\text{O})_2(\text{SO}_4)_3]\}$ (c) The two-dimensional 4×4 layer observed in **VII**.

the cyanosilylation of imines. We believe that the presence of Lewis acidity associated with the Cd center may be responsible for the observed catalytic behavior. Similar observations have also been made earlier.¹⁹



The compounds, after the reactions, were also examined using powder XRD for phase stability. The PXRD patterns did not show any appreciable change, which implies that the compounds are stable (see ESI,† Fig. S22, for compound **III**). This study suggests that cadmium thiosulfate hybrid compounds are not only stable, but also recyclable for catalytic purpose. The bound water molecules and the unsaturated Cd-coordination in **III** could have played a subtle role in the conversion of the imine, but this hypothesis needs to be confirmed by carrying out other related and detailed catalytic experiments.

Conclusions

The synthesis and structure of a new family of thiosulfate phases has been accomplished. The formation of one- and three-dimensional thiosulfate phases suggest that the thiosulfate compounds would also lead to a rich variety and diversity in the structures. The transformation reactions clearly reveal that the lower-dimensional structures are indeed reactive and can act as a precursor for phases of higher dimensionality. The close structural relationships between the three-dimensional structures and the transformation of one into another also suggest that the energy of formation of such structures could be comparable. The formation of cadmium sulfate phases during the transformation studies was unexpected, though with hindsight one can rationalize the formation of such phases. The preliminary catalytic conversion of the imines suggests that we are investigating a series of compounds with interesting possibilities. It would be desirable to prepare compounds that have three-dimensional connectivity arising entirely through the thiosulfate units as such structures could be distinctly different from the conventional ones. Efforts are under way towards this goal.

Experimental

Synthesis and initial characterization.

All the compounds were prepared by using self assembly methods (**I**, **III**) at room temperature or even lower and solvothermal conditions for the other compounds in a Teflon-lined autoclave. The reagents, Cd(NO₃)₂·4H₂O (Aldrich 98%), Na₂S₂O₃·5H₂O (Fluka 99%) and 4,4'-bipyridine (Aldrich 98%) were used as received without any further purification.

Synthesis of [Na₂(H₂O)₈][Cd(C₁₀H₈N₂)(S₂O₃)₂·2H₂O], **I.** A mixture of Cd(NO₃)₂·4H₂O (0.309 g, 1 mM) and Na₂S₂O₃·5H₂O (0.496 g, 2 mM) was dissolved in 3 ml of distilled water and 4,4'-bipyridine (0.156 g, 1 mM) was taken in 3 ml of EtOH. The alcoholic solution was layered carefully on top of the salt solution

and kept at 5 °C inside the refrigerator. Plate like crystals of **I** were obtained after ~72 h (yield = 90%).

Synthesis of [Cd(C₁₀H₈N₂)(HS₂O₃)₂][(C₁₀H₈N₂)₂·4H₂O], **II.** Cd(NO₃)₂·4H₂O (0.309 g, 1 mM) and Na₂S₂O₃·5H₂O (0.496 g, 2 mM) were dissolved in 3 ml of distilled water. Then, 4,4'-bipyridine (0.312 g, 2 mM) was added and the mixture was stirred continuously for 30 min at room temperature. This mixture was transferred into a 7 ml Teflon-lined stainless steel autoclave and heated at 75 °C for 60 h to result in block like crystals (yield = 70%).

Synthesis of [Cd(C₁₀H₈N₂)(H₂O)₂(S₂O₃)₂·2H₂O], **III.** A mixture of Cd(NO₃)₂·4H₂O (0.309 g, 1 mM) and Na₂S₂O₃·5H₂O (0.496 g, 2 mM) was dissolved in 3 ml of distilled water and 4,4'-bipyridine (0.156 g, 1 mM) was taken in 3 ml of EtOH. The alcoholic solution was layered carefully on top of the salt solution, similar to the synthesis of **I** and the mixture was allowed to evaporate slowly at room temperature (25 °C) to result in rod like crystals of **III** after ~60 h (yield = 90%).

Synthesis of [Cd₂(C₁₀H₈N₂)₂(S₂O₃)₂], **IV.** Cd(NO₃)₂·4H₂O (0.309 g, 1 mM) and Na₂S₂O₃·5H₂O (0.496 g, 2 mM) were dissolved in 3 ml of distilled water. Then, 4,4'-bipyridine (0.312 g, 2 mM) was added and the mixture was stirred continuously for 30 min at room temperature. This mixture was transferred into a 7 ml Teflon-lined autoclave and heated at 75 °C for 12 h to result in plate like crystals (yield = 90%).

Synthesis of [Cd₂(C₁₀H₈N₂)_{2.5}(S₂O₃)₂], **V.** Cd(NO₃)₂·4H₂O (0.309 g, 1 mM), Na₂S₂O₃·5H₂O (0.496 g, 2 mM) and 4,4'-bipyridine (0.312 g, 2 mM) were dissolved in 3 ml water. NH₄OH was slowly added to the mixture to obtain a pH of 8.0 and stirred for 30 min at room temperature. This mixture was transferred into a 7 ml Teflon-lined autoclave and heated at 75 °C for 60 h to result in rectangular block like crystals (yield = 85%).

Synthesis of [Cd₂(C₁₀H₈N₂)₂(H₂O)₃(SO₄)₂·2H₂O], **VI.** A mixture of Cd(NO₃)₂·4H₂O (0.309 g, 1 mM), Na₂SO₄ (0.142 g, 1 mM) and 4,4'-bipyridine (0.156 g, 1 mM) was dissolved in 3 ml of distilled water and heated at 75 °C for 60 h to result in block like crystals.

Synthesis of [Cd(C₁₀H₈N₂)(SO₄)], **VII.** A mixture of Cd(NO₃)₂·4H₂O (0.309 g, 1 mM) and Na₂SO₄ (0.142 g, 1 mM) was dissolved in 1.5 ml of distilled water and 4,4'-bipyridine (0.156 g, 1 mM) was taken in 1.5 ml of EtOH. The alcoholic solution was mixed with the water mixture and heated in a 7 ml Teflon-lined autoclave at 110 °C for 60 h resulting in plate like crystals.

The synthetic compositions and conditions employed for the preparation of the phases are given in Table 1. Elemental analyses were carried out using a Thermo Finnigan FLASH EA 1112 CHN analyzer (Table 1).

All the compounds were characterized by powder X-ray diffraction (XRD), IR, UV-visible and TGA studies. The powder XRD patterns were recorded in the 2θ range 5–50° by using Cu Kα radiation (Philips, X'pert-Pro). The XRD patterns indicated that the products were new and the patterns were entirely consistent with the simulated XRD pattern generated based on the structures determined using the single-crystal XRD (see ESI,† Fig. S1–S7). Infrared (IR) spectroscopic studies have been carried out in the mid-IR region (4000 to 400 cm^{−1}) on KBr pellets (Perkin Elmer,

SPECTRUM 1000). IR spectra of all the compounds were more or less similar and can be described in terms of five distinct regions (see ESI,† Fig. S8). (i) Compounds **I**, **II**, **III** and **VI** have bands at 3600–3300 cm⁻¹, dominated by a broad band centered at 3435 cm⁻¹ indicative of the presence of water molecules. A band at 3375 cm⁻¹ can be assigned to the protonated OH group of the thiosulfate unit in **II**; (ii) a band at 3045 cm⁻¹ can be assigned to aromatic $\nu(\text{CH})$ modes of the bipyridine ring; (iii) a band in the region 1650–1200 cm⁻¹ can be assigned to the C–H bending vibrations due to the asymmetric and symmetric modes of the pyridine skeletal; (iv) 1150–1000 cm⁻¹ region, with sharp band at 1130 cm⁻¹ is due to ν_s (S–O) and (v) the bands in the region of 805–535 cm⁻¹ are due to the bending mode of S–O and ν_s (S–S) of the thiosulfate unit.

The solid state UV-visible absorbance spectroscopic studies were carried out for all compounds **I–VII** at room temperature using a Perkin-Elmer model Lambda 35 UV-visible spectrometer (see ESI,† Fig. S9). The surface area of the three thiosulfate compounds (**III**, **IV** and **V**) was determined using porosimeter (Belsorp, Japan) in the presence of N₂. The adsorption–desorption isotherm has shown that the compounds are very less porous. Compound **III** has the highest surface area (3 m² g⁻¹) than compounds **IV** and **V** (1.4 m² g⁻¹ and 1.3 m² g⁻¹, respectively, see ESI,† Fig. S10).

Single-crystal structure determination

A suitable single-crystal of each compound was carefully selected under a polarizing microscope and glued to a thin glass fiber

with a cyanoacrylate (super glue) adhesive. Single-crystal data were collected on a Bruker AXS smart Apex CCD diffractometer at 293(2) K. The X-ray generator was operated at 50 kV and 35 mA using Mo K α ($\lambda = 0.71073$ Å) radiation. Data were collected with ω scan width of 0.3°. A total of 606 frames were collected at three different settings of ϕ (0, 90, 180°) keeping the sample-to-detector distance fixed at 6.03 cm and the detector position (2θ) fixed at -25° . The data were reduced using SAINTPLUS,²⁰ and an empirical absorption correction was applied using the SADABS program.²¹ The structure was solved and refined using SHELXL97²² present in the WinGx suit of programs (Version 1.63.04a).²³ The hydrogen positions of the two lattice water molecules and eight coordinated water molecules of the sodium, present in compound **I**, could not be located. All the hydrogen positions of the 4,4'-bipyridine for the compounds and the hydrogen position of the hydroxyl group in **II** could be located but the hydrogen positions of the four lattice water molecules in **II**, the hydrogen positions of one lattice water molecule in **III**, two lattice water molecules and three coordinated water molecules in **VI** could not be located. Where the hydrogen positions were located, restraints for the bond distances were used during the refinement to keep the hydrogen atoms bonded with the three water molecules in **III**. The hanging thiosulfate groups in **I** appear to be disordered with a mixed occupancy of 70 : 30 (see ESI†). The corresponding positions were refined isotropically. Full-matrix least-squares refinement against $|F^2|$ was carried out using the WinGx package of programs. Details of the structure solution and final refinements for all the structures are given in Table 2.

Table 2 Crystal data and structure refinement parameters for **I–VII**

Structural parameter	I	II	III	IV	V	VI	VII
Empirical formula	[Na ₂ (H ₂ O) ₈]-[Cd(C ₁₀ H ₈ N ₂)(S ₂ O ₃) ₂]-2H ₂ O	[Cd ₂ (C ₁₀ H ₈ N ₂) ₂ -(HS ₂ O ₃) ₂ (S ₂ O ₃) ₂]-[(C ₁₀ H ₉ N ₂) ₂ (C ₁₀ H ₈ N ₂) ₂]-8H ₂ O	[Cd(C ₁₀ H ₈ N ₂)(H ₂ O) ₂ -(S ₂ O ₃) ₂]-2H ₂ O	[Cd(C ₁₀ H ₈ N ₂) _{1.5} -(S ₂ O ₃) ₂]	[Cd ₂ (C ₁₀ H ₈ N ₂)(S ₂ O ₃) ₂]	[Cd ₂ (C ₁₀ H ₈ N ₂) ₂ -(H ₂ O) ₃ (SO ₄) ₂]-2H ₂ O	[Cd(C ₁₀ H ₈ N ₂)(SO ₄) ₂]
Formula weight	718.85	1758.42	452.75	458.80	839.50	819.28	364.64
Crystal system	Monoclinic	Monoclinic	Monoclinic	Monoclinic	Monoclinic	Monoclinic	Tetragonal
Space group	<i>P</i> 2 ₁ (No. 4)	<i>P</i> 2 ₁ / <i>n</i> (No. 13)	<i>P</i> 2 ₁ / <i>n</i> (No. 14)	<i>C</i> 2/ <i>c</i> (No. 15)	<i>P</i> 2 ₁ / <i>c</i> (No. 14)	<i>C</i> 2 (No. 5)	<i>P</i> 4 ₂ / <i>m</i> (No. 113)
<i>a</i> /Å	6.9673(2)	13.420(3)	7.1760(13)	12.628(2)	11.0343(17)	24.5534(6)	6.8212(7)
<i>b</i> /Å	14.1333(4)	17.361(4)	10.5145(18)	15.081(2)	15.894(2)	9.7877(2)	6.8212(7)
<i>c</i> /Å	14.3657(4)	15.840(3)	20.899(4)	17.362(3)	15.823(2)	13.5716(3)	11.838(2)
α /°	90.000	90.000	90.000	90.000	90.000	90.000	90.000
β /°	104.0350(10)	105.228(3)	99.300(3)	107.076(3)	91.969(3)	120.579(2)	90.000
γ /°	90.000	90.000	90.000	90.000	90.000	90.000	90.000
<i>V</i> /Å ³	1372.37(7)	3560.8(12)	1556.1(5)	3160.8(9)	2773.3(7)	2807.96(11)	550.81(14)
<i>Z</i>	2	2	4	8	4	4	2
<i>D</i> _{calc} /g cm ⁻³	1.691	1.625	1.924	1.928	2.011	1.914	2.199
μ /mm ⁻¹	1.198	0.911	1.705	1.665	1.887	1.733	2.179
λ (Mo K α)/Å	0.71073	0.71073	0.71073	0.71073	0.71073	0.71073	0.71073
θ range/°	2.05–30.67	1.96–28.07	2.17–26.37	2.16–28.08	1.82–28.08	1.74–30.57	1.72–26.30
Total data collected	14 333	37 720	12 147	13 654	23 968	30 229	4320
Unique data	7626	8352	3160	3729	6541	8579	627
<i>R</i> _{int}	0.0487	0.0357	0.0249	0.0305	0.0310	0.0417	0.1463
Flack parameter	0.00(1)					−0.03(4)	0.0(3)
<i>R</i> indexes [<i>I</i> > 2 σ (<i>I</i>)]	<i>R</i> ₁ = 0.0630 <i>wR</i> ₂ = 0.1632	<i>R</i> ₁ = 0.0677 <i>wR</i> ₂ = 0.1585	<i>R</i> ₁ = 0.0323 <i>wR</i> ₂ = 0.0792	<i>R</i> ₁ = 0.0332 <i>wR</i> ₂ = 0.0700	<i>R</i> ₁ = 0.0372 <i>wR</i> ₂ = 0.0646	<i>R</i> ₁ = 0.0485 <i>wR</i> ₂ = 0.1311	<i>R</i> ₁ = 0.0451 <i>wR</i> ₂ = 0.0792
<i>R</i> indexes (all data)	<i>R</i> ₁ = 0.0689 <i>wR</i> ₂ = 0.1687	<i>R</i> ₁ = 0.1060 <i>wR</i> ₂ = 0.1814	<i>R</i> ₁ = 0.0374 <i>wR</i> ₂ = 0.0823	<i>R</i> ₁ = 0.0433 <i>wR</i> ₂ = 0.0742	<i>R</i> ₁ = 0.0558 <i>wR</i> ₂ = 0.0705	<i>R</i> ₁ = 0.0687 <i>wR</i> ₂ = 0.1435	<i>R</i> ₁ = 0.0503 <i>wR</i> ₂ = 0.0812

$R_1 = \sum \|F_o| - |F_c|\| / \sum |F_o|$; $wR_2 = \{\sum [w(F_o^2 - F_c^2)^2] / \sum [w(F_o^2)^2]\}^{1/2}$. $w = 1/[\sigma^2(F_o^2) + (aP)^2 + bP]$, $P = [\max(F_o^2, 0) + 2(F_c^2)]/3$, where $a = 0.0501$ and $b = 6.0399$ for **I**, $a = 0.0661$ and $b = 15.5599$ for **II**, $a = 0.0379$ and $b = 2.3594$ for **III**, $a = 0.0277$ and $b = 3.3819$ for **IV**, $a = 0.0213$ and $b = 2.1270$ for **V**, $a = 0.0762$ and $b = 7.0806$ for **VI**, and $a = 0.0275$ and $b = 0.4698$ for **VII**.

The selected bond distances and angles are given in Tables S1–S7 (see ESI†) for all the structures. The observed hydrogen bond interactions are listed in Table S8 for compounds **I**, **II** and **III**. The crystallographic data for compounds can be found in the ESI.†

Thermal studies

TGA studies (Mettler-Toledo TG850) of all the compounds were carried out in an atmosphere of flowing oxygen (flow rate = 50 mL min^{−1}) in the temperature range 30–800 °C (heating rate = 2 °C min^{−1}). The results of the TGA studies (see ESI,† Fig. S11) are summarized in Table S11 (see ESI†).

Acknowledgements

The authors thank Mr Udishnu Sanyal and Prof. B. R. Jagirdar of the Department of Inorganic and Physical Chemistry, Indian Institute of Science, for help with the catalytic studies. The authors thank the Department of Science and Technology (DST), Government of India, for the award of a research grant. The Council of Scientific and Industrial Research (CSIR), Government of India, is thanked for the award of a research grant (SN) and a fellowship (AKP). SN thanks DST for the award of a RAMANNA fellowship.

References

- (a) J. M. Thomas, *Angew. Chem., Int. Ed.*, 1999, **38**, 3588; (b) A. Muller, H. Reuter and S. Dillinger, *Angew. Chem., Int. Ed. Engl.*, 1995, **34**, 2328; (c) P. J. Hagrman, D. Hagrman and J. Zubietta, *Angew. Chem., Int. Ed.*, 1999, **38**, 2638; (d) D. MasPOCH, D. Ruiz-Molina and J. Vaciána, *Chem. Soc. Rev.*, 2007, **36**, 770.
- (a) A. K. Cheetham, G. Férey and T. Loiseau, *Angew. Chem., Int. Ed.*, 1999, **38**, 3268; (b) S. Natarajan and S. Mandal, *Angew. Chem., Int. Ed.*, 2008, **47**, 4798; (c) C. N. R. Rao, S. Natarajan, A. Choudhury, S. Neeraj and A. A. Ayi, *Acc. Chem. Res.*, 2001, **34**, 80; (d) S. T. Wilson, B. M. Lok, C. A. Messina, T. R. Cannan and E. M. Flanigen, *J. Am. Chem. Soc.*, 1982, **104**, 1146.
- C. N. R. Rao, J. N. Behra and M. Dan, *Chem. Soc. Rev.*, 2006, **35**, 375.
- (a) M. E. D. d. Vivar, S. Baggio, M. T. Garland and R. Baggio, *Acta Crystallogr., Sect. C: Cryst. Struct. Commun.*, 2007, **63**, m123; (b) M. Harvey, S. Baggio, H. Pardo and R. Baggio, *Acta Crystallogr., Sect. C: Cryst. Struct. Commun.*, 2004, **60**, m79; (c) E. Freire, S. Baggio, R. Baggio and A. Mombru, *Acta Crystallogr., Sect. C: Cryst. Struct. Commun.*, 2001, **57**, 14.
- (a) W.-J. Chang, Y.-C. Jiang, S.-L. Wang and K.-H. Lii, *Inorg. Chem.*, 2006, **45**, 6586; (b) L.-H. Huang, H.-M. Kao and K.-H. Lii, *Inorg. Chem.*, 2002, **41**, 2936; (c) L.-I. Hung, S.-L. Wang, H.-M. Kao and K.-H. Lii, *Inorg. Chem.*, 2002, **41**, 3929; (d) W.-K. Chang, R.-K. Chiang, Y.-C. Jiang, S.-L. Wang, S.-F. Lee and K.-H. Lii, *Inorg. Chem.*, 2004, **43**, 2564.
- (a) P. Mahata, M. Prabu and S. Natarajan, *Inorg. Chem.*, 2008, **47**, 8451; (b) P. Mahata, A. Sundaresan and S. Natarajan, *Chem. Commun.*, 2007, 4471; (c) A. J. Bailey, C. Lee, R. K. Feller, J. B. Orton, C. M. Draznieks, B. Slater, W. T. A. Harrison, P. Simoncic, A. Navrotsky, M. C. Grossel and A. K. Cheetham, *Angew. Chem., Int. Ed.*, 2008, **47**, 8634; (d) A. K. Cheetham, C. N. R. Rao and R. K. Feller, *Chem. Commun.*, 2006, 4780.
- A. K. Paul, G. Madras and S. Natarajan, *CrystEngComm*, 2009, **11**, 55.
- S. D. Huang, R.-G. Xiong, J. Han and B. R. Weiner, *Inorg. Chim. Acta*, 1999, **294**, 95.
- (a) G. R. Desiraju, *Angew. Chem., Int. Ed. Engl.*, 1995, **34**, 2311; (b) *Perspectives in Supramolecular Chemistry: The Crystal as a Supramolecular Entity*, ed. G. R. Desiraju, Wiley, Chichester, 1996, vol. 2.
- O. Fabelo, J. Pasán, L. Canadillas-Delgado, F. S. Delgado, A. Labrador, F. Lloret, M. Julve and C. Ruiz-Pérez, *CrystEngComm*, 2008, **10**, 1743.
- (a) V. A. Blatov, 2006, <http://www.topos.ssu.samara.ru/>; (b) V. A. Blatov, A. P. Shevchenko and V. N. Serezhkin, *J. Appl. Crystallogr.*, 2000, **33**, 1193.
- L. Ohrstrom and K. Larsson, *Molecule-Based Materials-The Structural Network Approach*, Elsevier, 2005.
- A. M. Kutasi, A. R. Harris, S. R. Batten, B. Moubaraki and K. S. Murray, *Cryst. Growth Des.*, 2004, **4**, 605.
- A. A. Ayi, A. Choudhury, S. Natarajan, S. Neeraj and C. N. R. Rao, *J. Mater. Chem.*, 2001, **11**, 1181.
- A. Choudhury, S. Neeraj, S. Natarajan and C. N. R. Rao, *J. Mater. Chem.*, 2001, **11**, 1537.
- V. K. Rao, S. Chakrabarti and S. Natarajan, *Inorg. Chem.*, 2007, **46**, 10781.
- G. Paul, A. Choudhury and C. N. R. Rao, *J. Chem. Soc., Dalton Trans.*, 2002, 3859.
- C.-Y. Chen, K.-H. Lii and A. J. Jacobson, *J. Solid State Chem.*, 2003, **172**, 252.
- O. Ohmori and M. Fujita, *Chem. Commun.*, 2004, 1586.
- SMART (V 5.628)*, *SAINT (V 6.45a)*, *XPRED*, *SHELXTL*, Bruker AXS Inc. Madison, Wisconsin, USA, 2004.
- G. M. Sheldrick, *Siemens Area Detector Absorption Correction Program*, University of Göttingen, Göttingen, Germany, 1994.
- G. M. Sheldrick, *SHELXL-97 Program for Crystal Structure Solution and Refinement*, University of Göttingen, Göttingen, Germany, 1997.
- J. L. Farrugia, WinGx suite for small-molecule single crystallography, *J. Appl. Crystallogr.*, 1999, **32**, 837.